MARINE SCIENCE & ENGINEERING WITH PLYMOUTH UNIVERSITY

The University of Plymouth

MODELLING WITH PLYMOUTH UNIVERSITY

A-type and B-type internal solitary waves in the northern South China Sea

Vasiliy Vlasenko[a] , *Chuncheng Guo*[a,b] and Nataliya Stashchuk[a]

[a]School of Marine Science and Engineering, University of Plymouth, UK
[b]College of Physical and Environmental Oceanography, Ocean University of China, China

OUTLOOK:

1. Motivation
•Introduction into the problem
•The area
•Some preliminary results
•Observational evidence of A and B internal waves

2. Analysis of some historical data

3. MITgcm modelling of A and B internal waves
•Model set-up
•Comparison with observational data

4. Analysis and interpretation of the model results
   - Generation mechanism
   - Multi-harmonic solution
   - Evolutionary mechanism

5. Conclusions

1. Motivation

Generation Mechanism

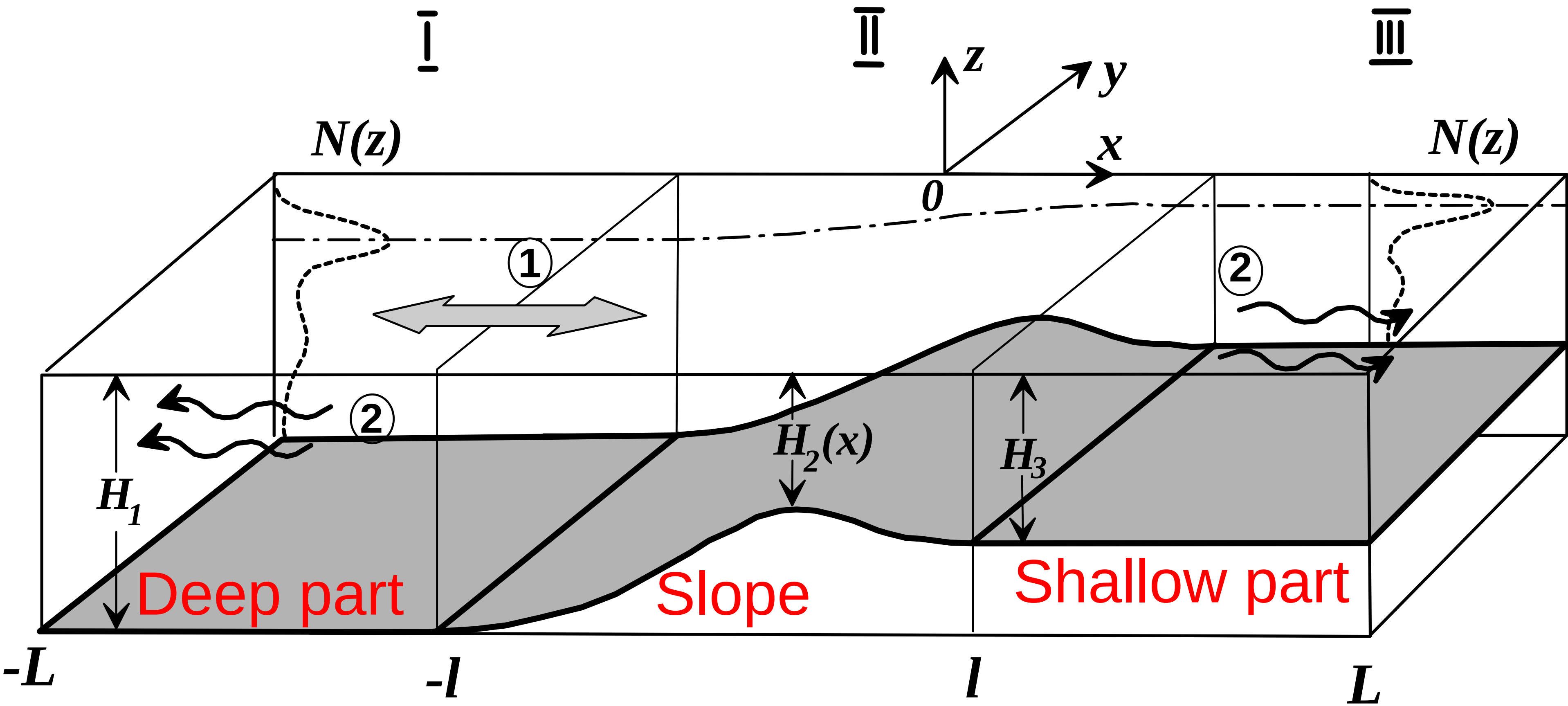

1 Tidal wave

2 Internal waves

1. Motivation

Generation of nonlinear internal waves

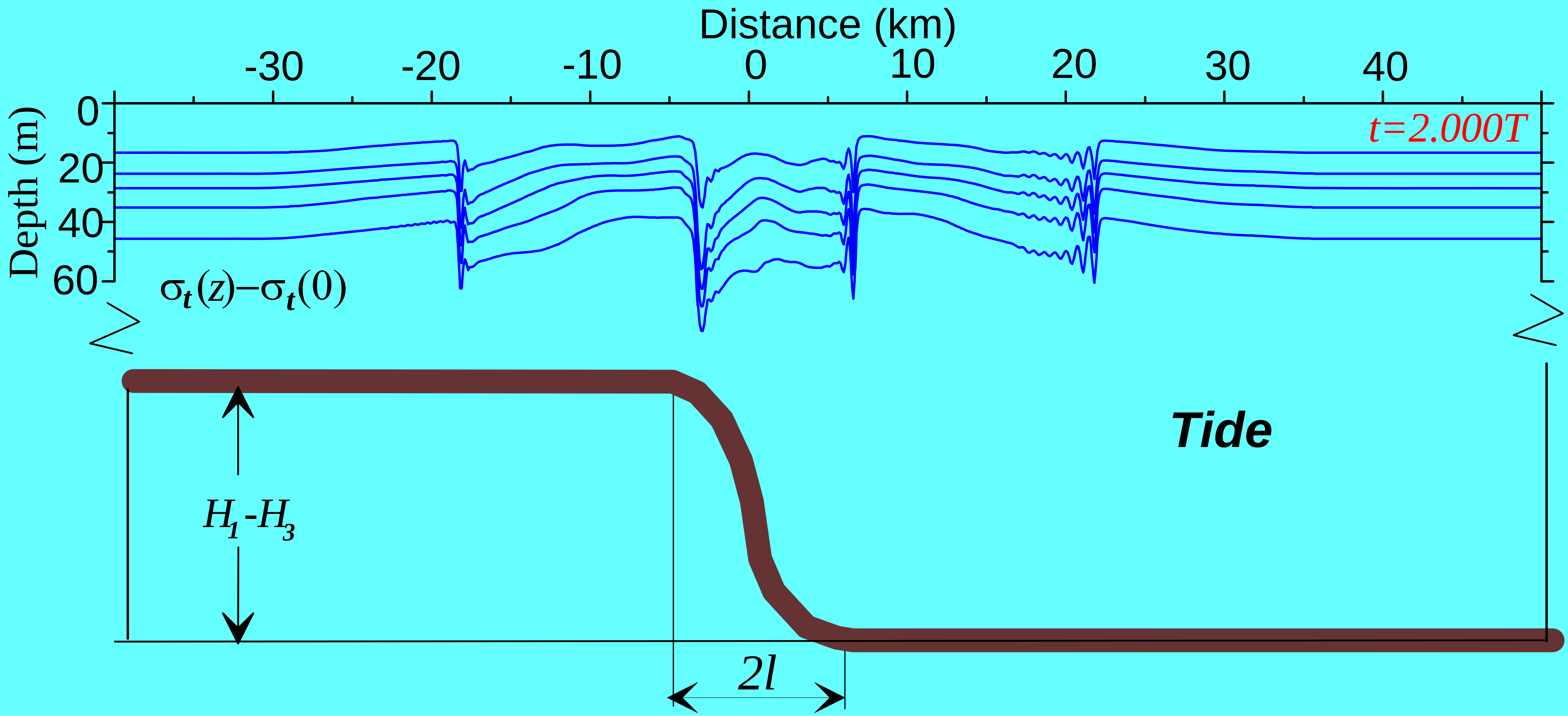

1. Motivation

The area

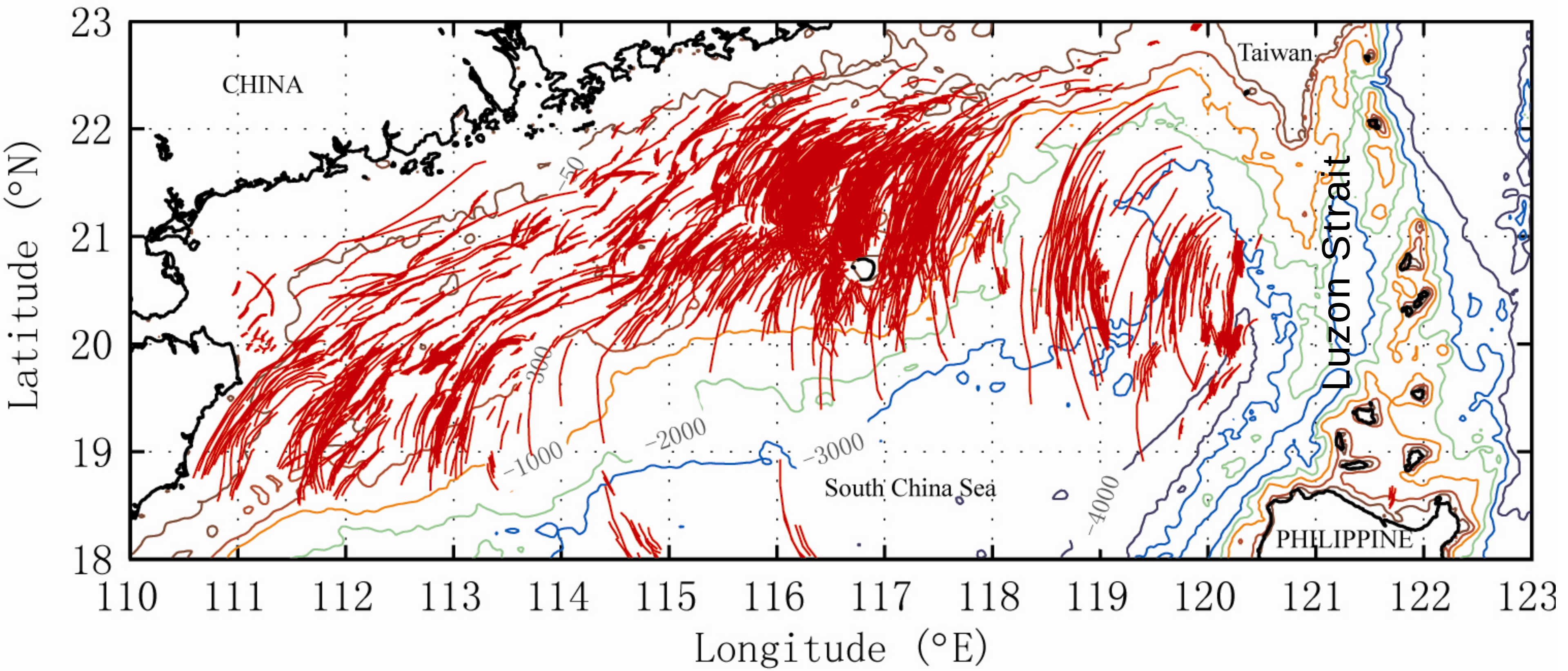

1. Motivation

Statistical analysis of SAR images from 1995-2001 (Zheng et al., 2007)

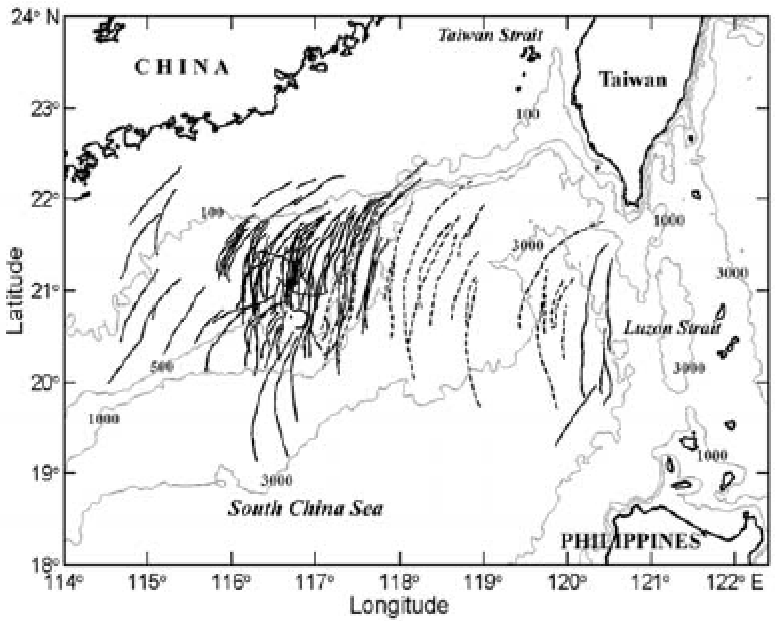

Zhao et al. (2004) compiled a spatial distribution by overlapping their signatures

Single internal wave packet (width 2.5 km)

Multiple internal wave Packets with (width 0.8 km

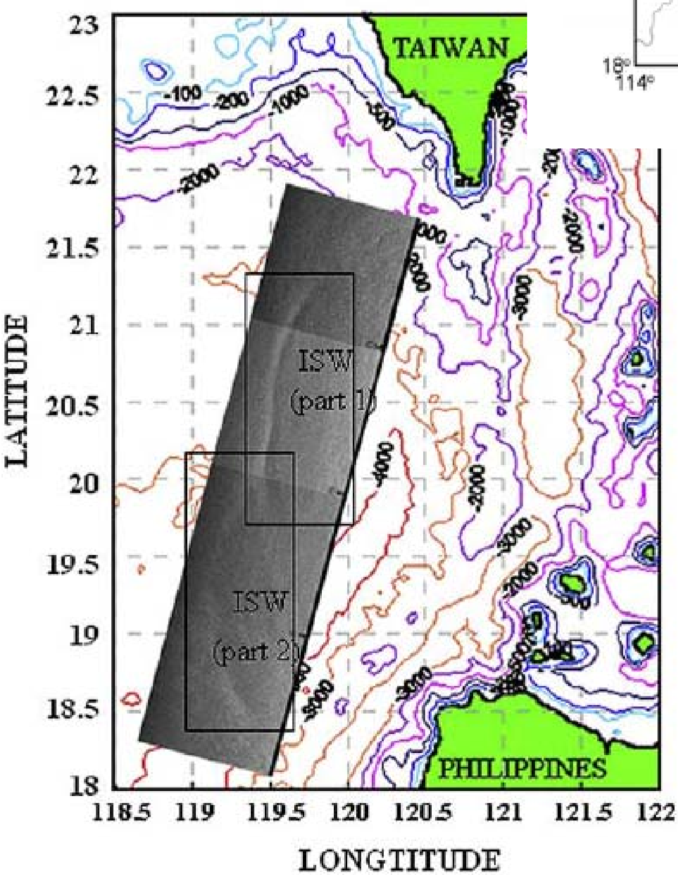

Two types of solitary Waves have been identified between 118° and the west of the Luzon Strait

Two types of ISWs

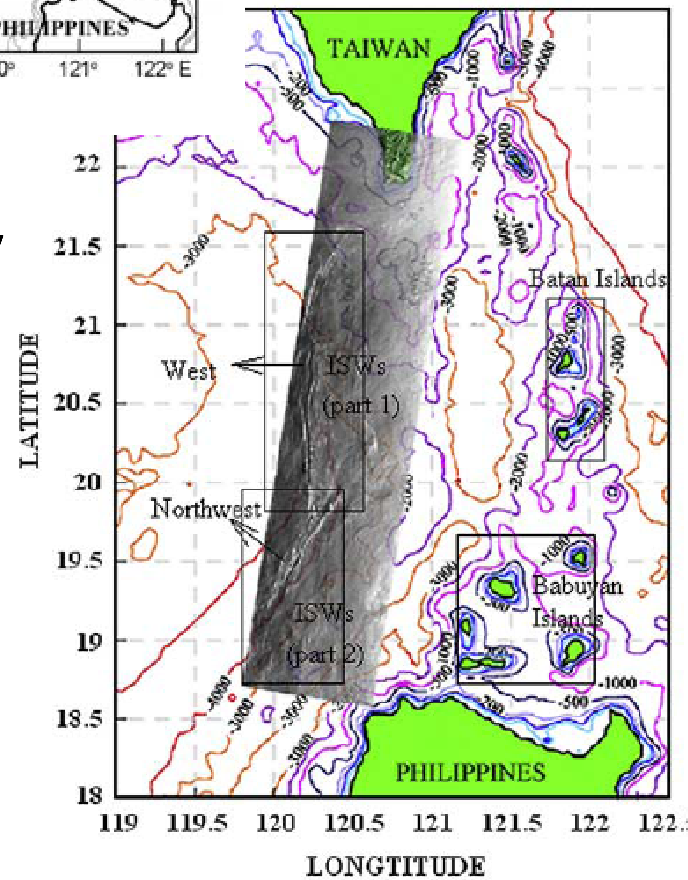

1. Motivation

Preliminary Study

Bottom topography of the Luzon Strait with schematic presentation of multiple wave packets and solitary waves. White rectangle is the model domain $L_x \times L_y = 670 \times 134$ km^2

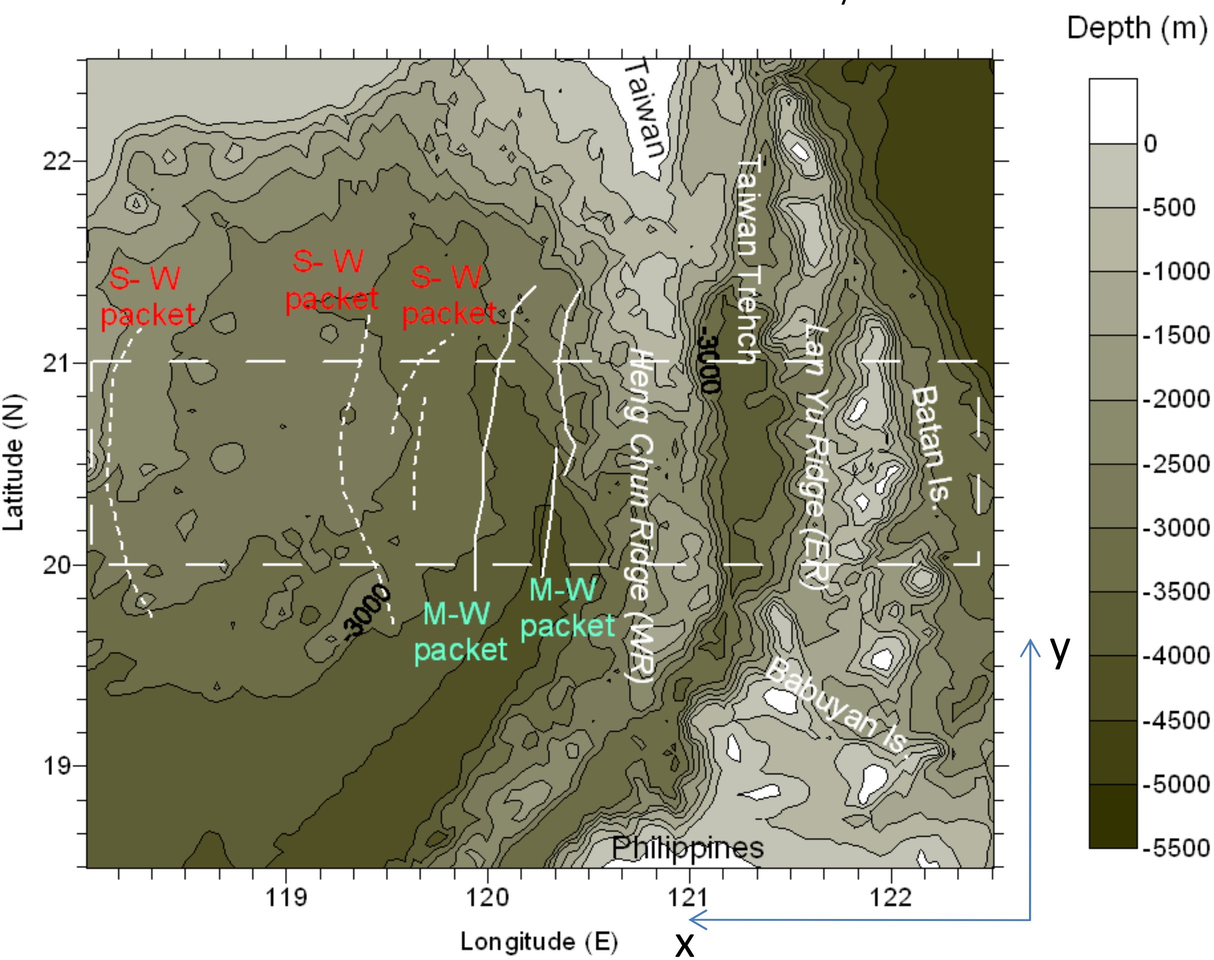

Averaged temperature and salinity

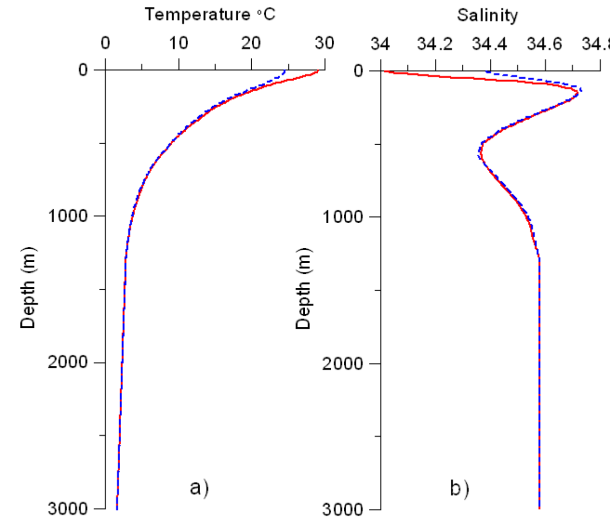

MITgcm is used

Grid in horizontal directions

$\Delta x = 250$ m; $\Delta y = 1000$ m

Grid in vertical direction:

$\Delta z = 10$ m in upper 500 m

$\Delta z = 50$ m in the rest of water

Vlasenko, V., Stashchuk, N., Guo, C., Chen, X., 2010. Multimodal structure of baroclinic tides in the South China Sea. Nonlinear Processes in Geophysics 17, 529-543.

Preliminary Study

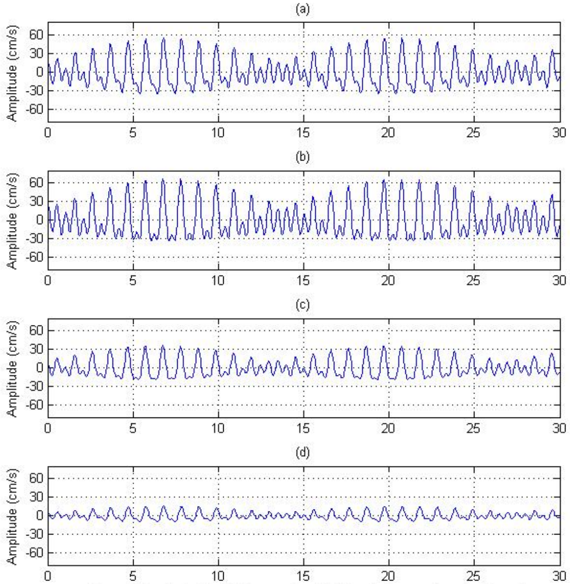

Figure2 Zonal velocities(u) in a month at 4 different sites as shown in Figure1:

Zonal velocities in a month at different cites

The tidal dynamics is governed by a superposition of eight principal tidal harmonics: M2, S2, K1, O1, N2, K2, P1, Q1 (Egbert and Erofeeva, 2002). Zu et al. (2008) have shown That the model output for eight harmonics is similar to output with only two of them M2 and K1.

Forcing:

$$F_x = UH_0 / H(x,y)\sigma\cos(\sigma t); \qquad F_y = UH_0 / H(x,y) f \sin(\sigma t).$$

M_2

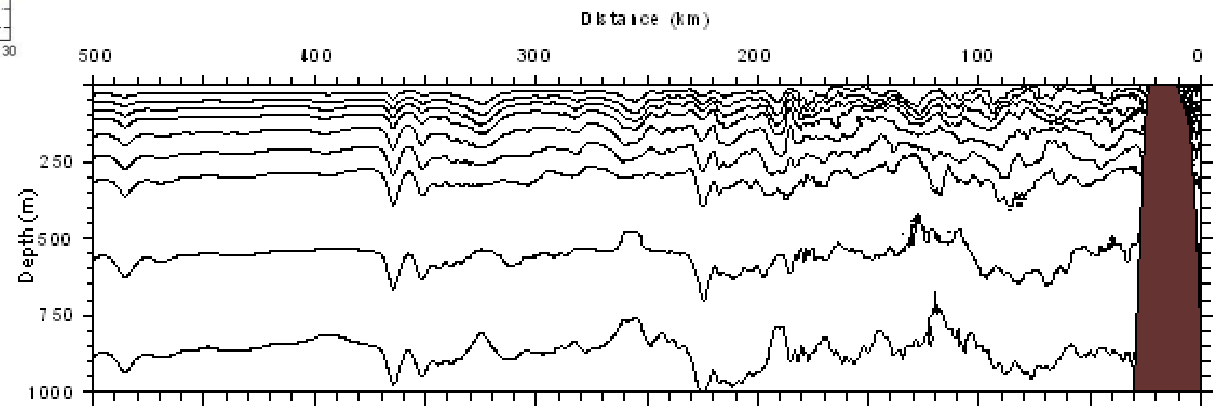

K_1

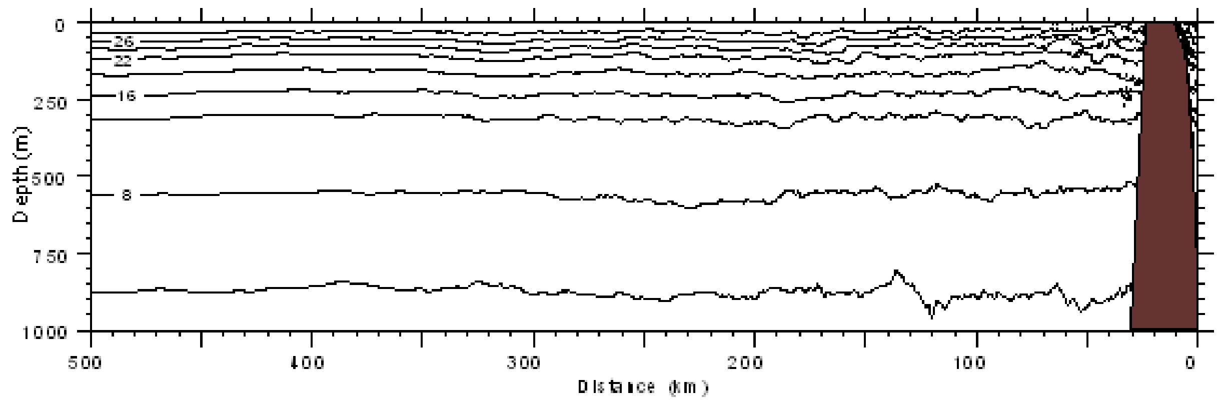

3D modelling of baroclinic tides using nonhydrostatic MITgcm

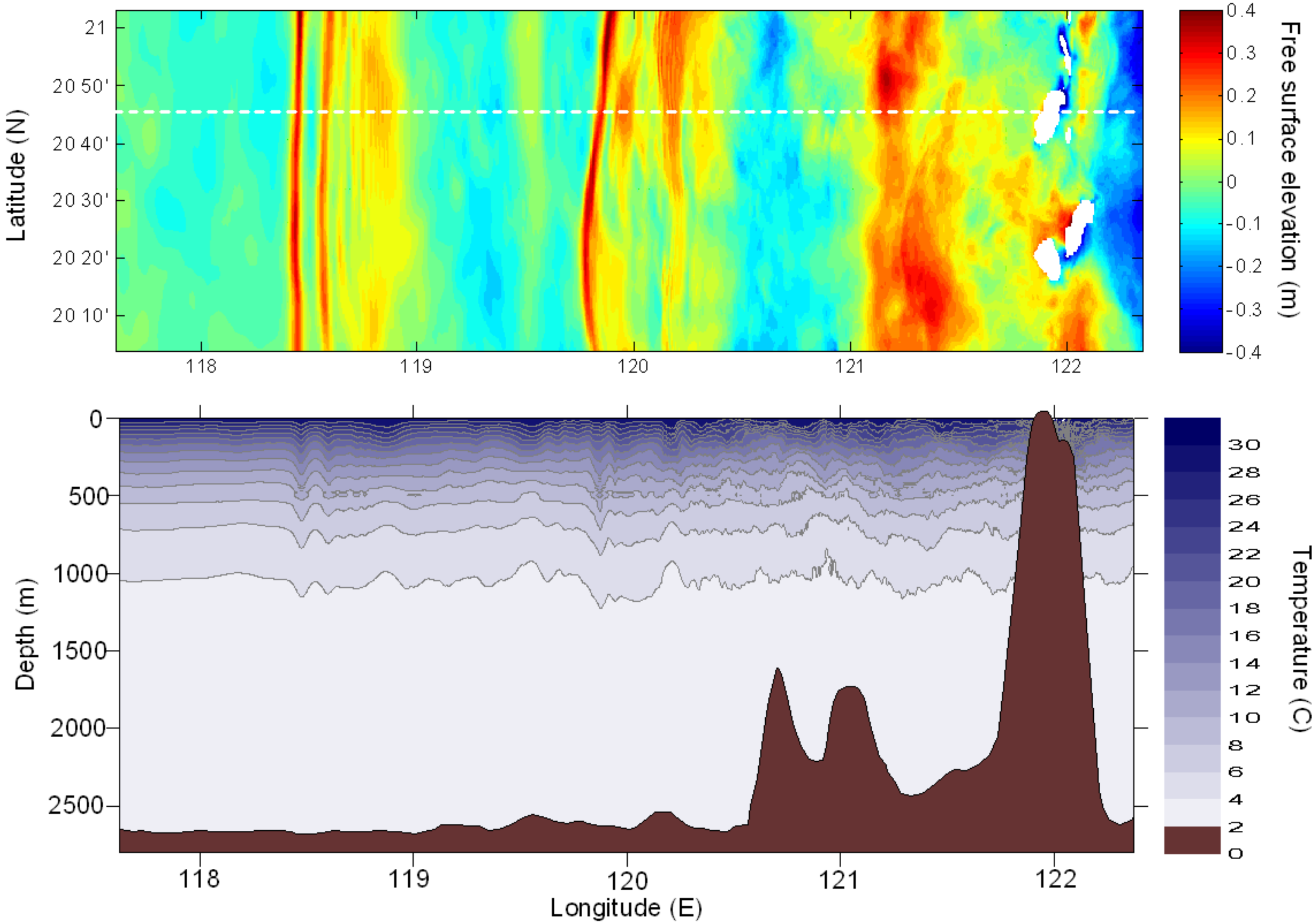

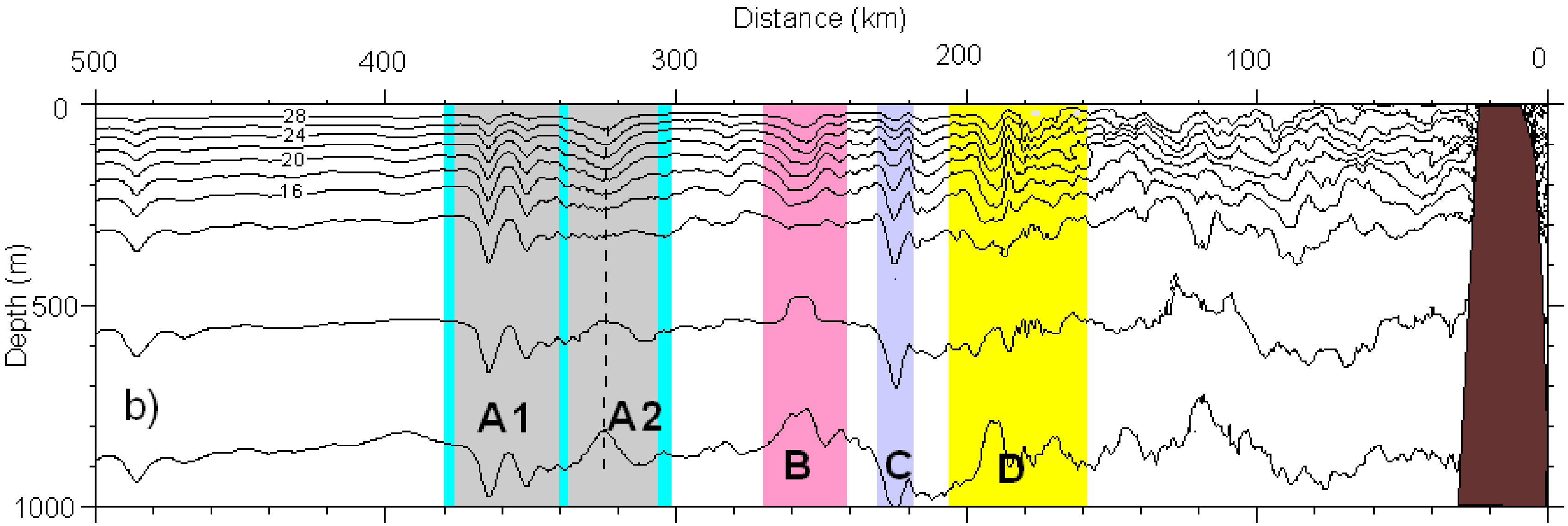

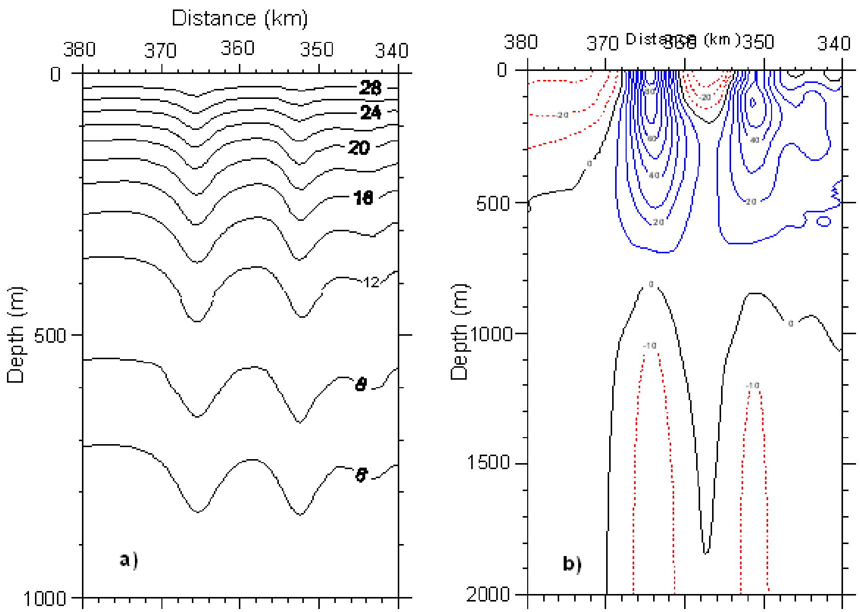

A1

A pair of first-mode solitary waves (rectangle A1)

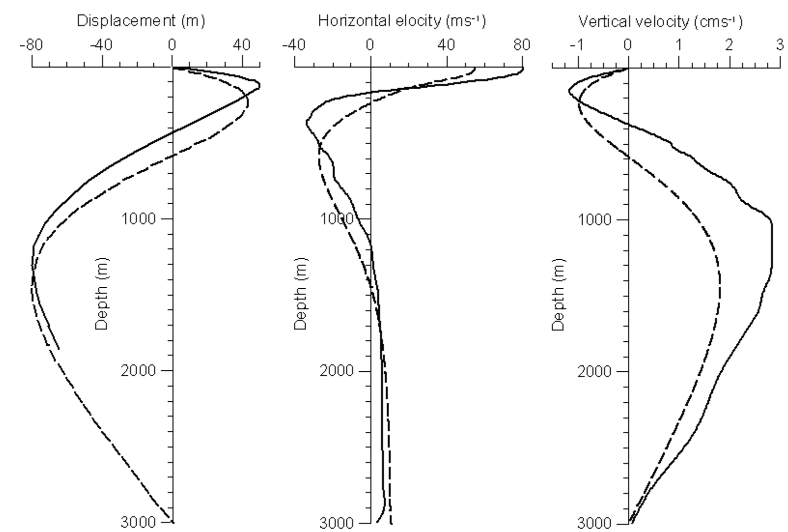

Vertical profile of a second-mode solitary Waves in its centre (fragment A2)

——— numerical model; - - - - - - - BVP

1. Motivation

Observational evidence of A-type and B-type internal waves

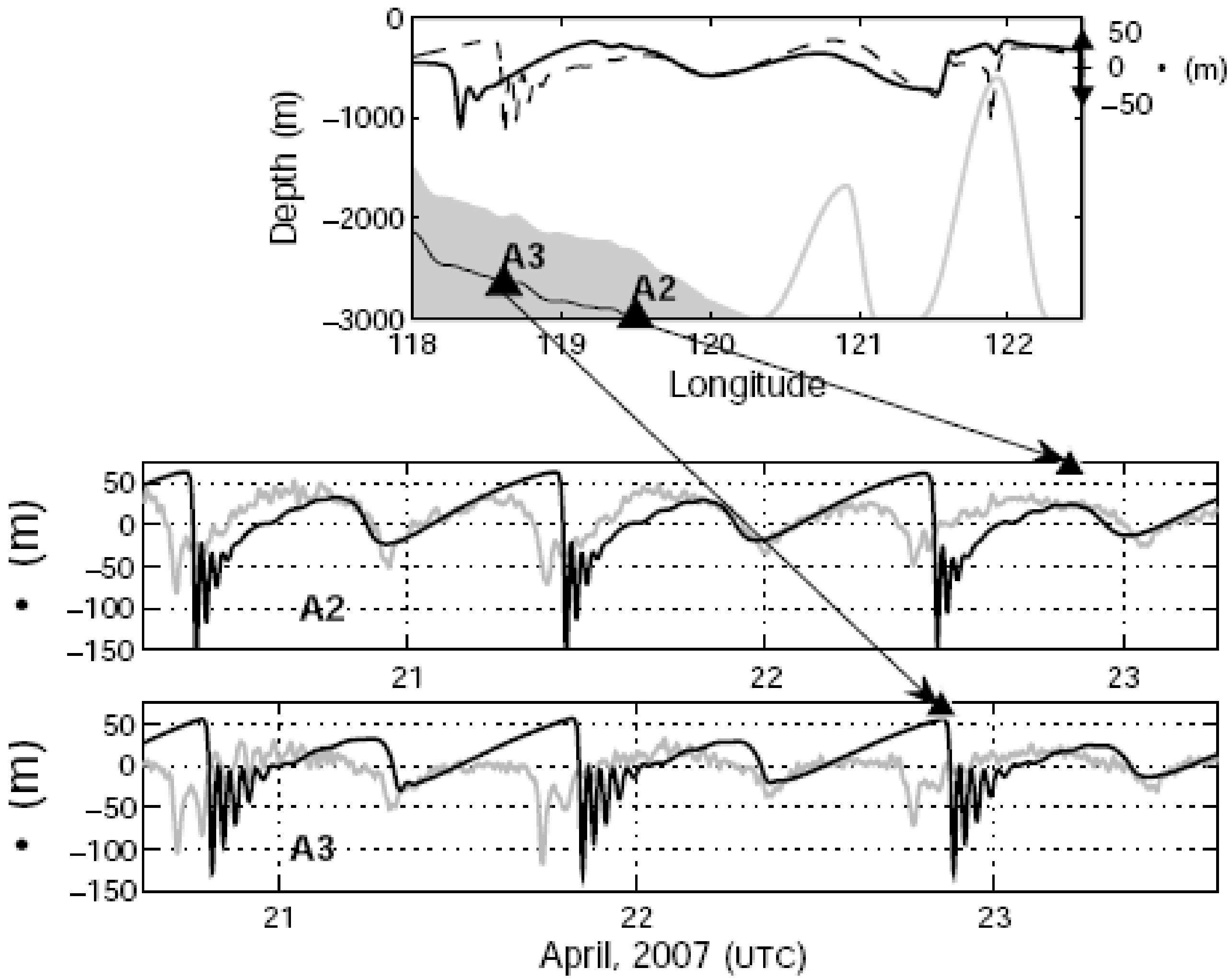

Farmer, D., Li, Q., Park, J.-H., 2009. Internal wave observations in the South China Sea: the role of rotation and non-linearity. Atmos.-Ocean 47(4), 267-280.

1. Motivation

Observational evidence of A-type and B-type internal waves

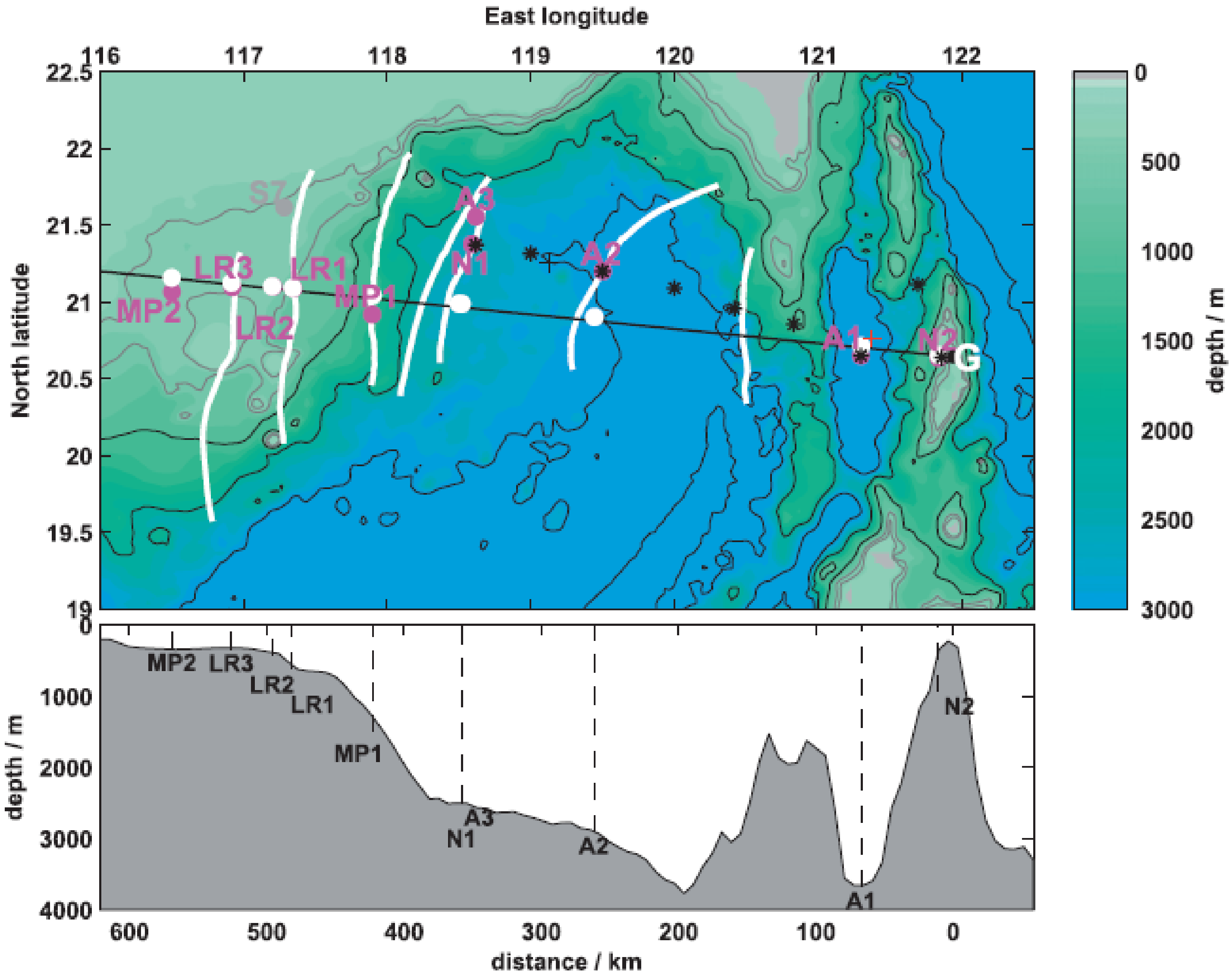

Alford, M., Lien, R., Simmons, H., Klymak, J., Ramp, S., Yang, Y., Tang, D., Chang, M., 2010. Speed and evolution of nonlinear internal waves transiting the South China Sea. JPO, 40,1338-

Observational evidence of A-type and B-type internal waves

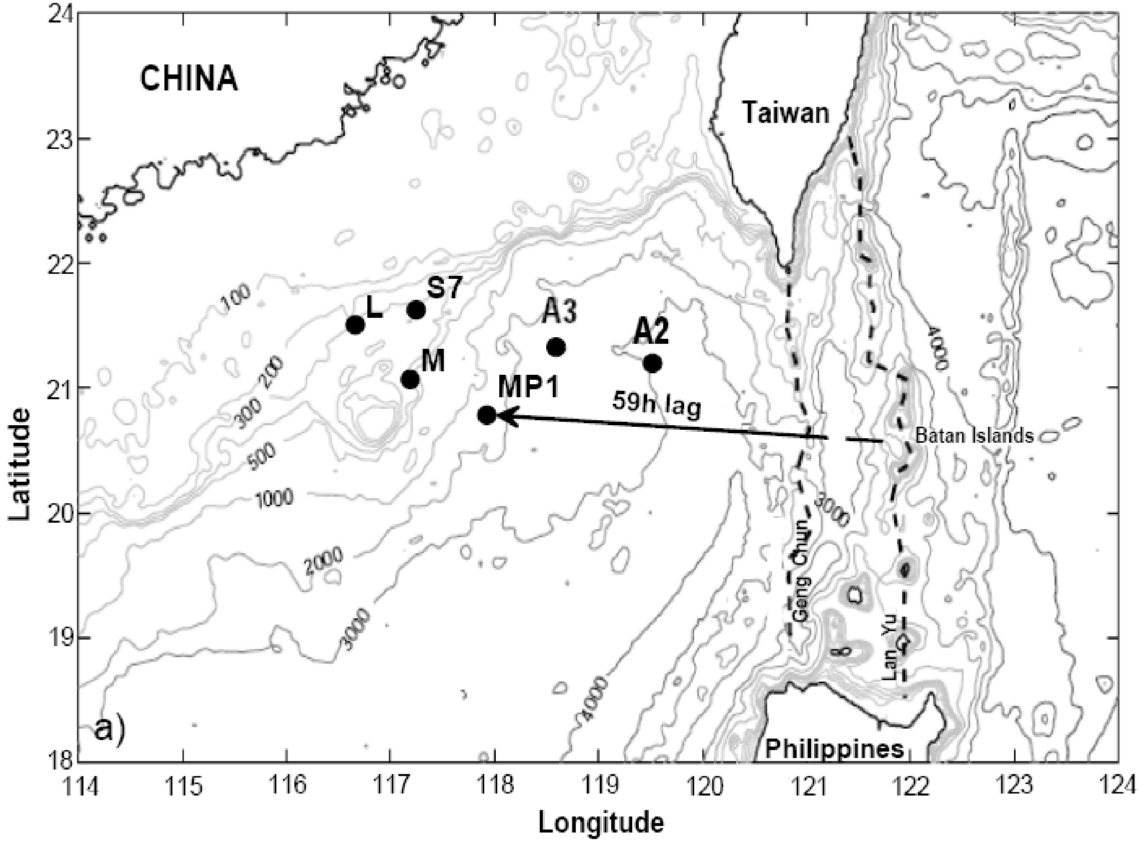

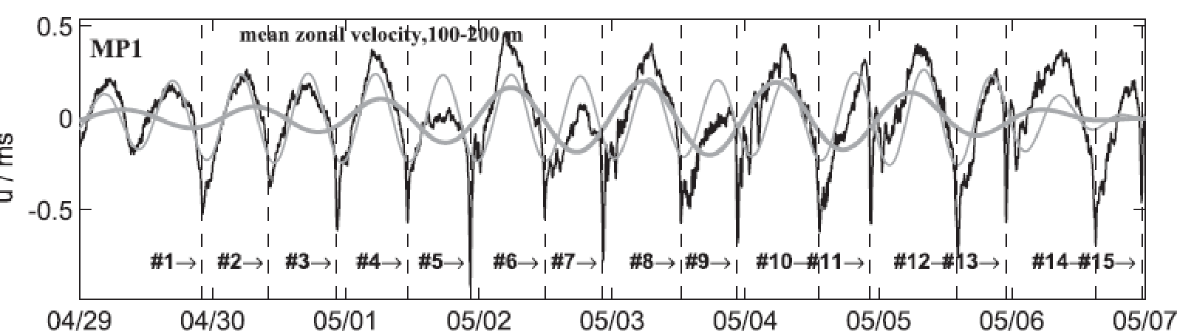

ADCP data at point MP1

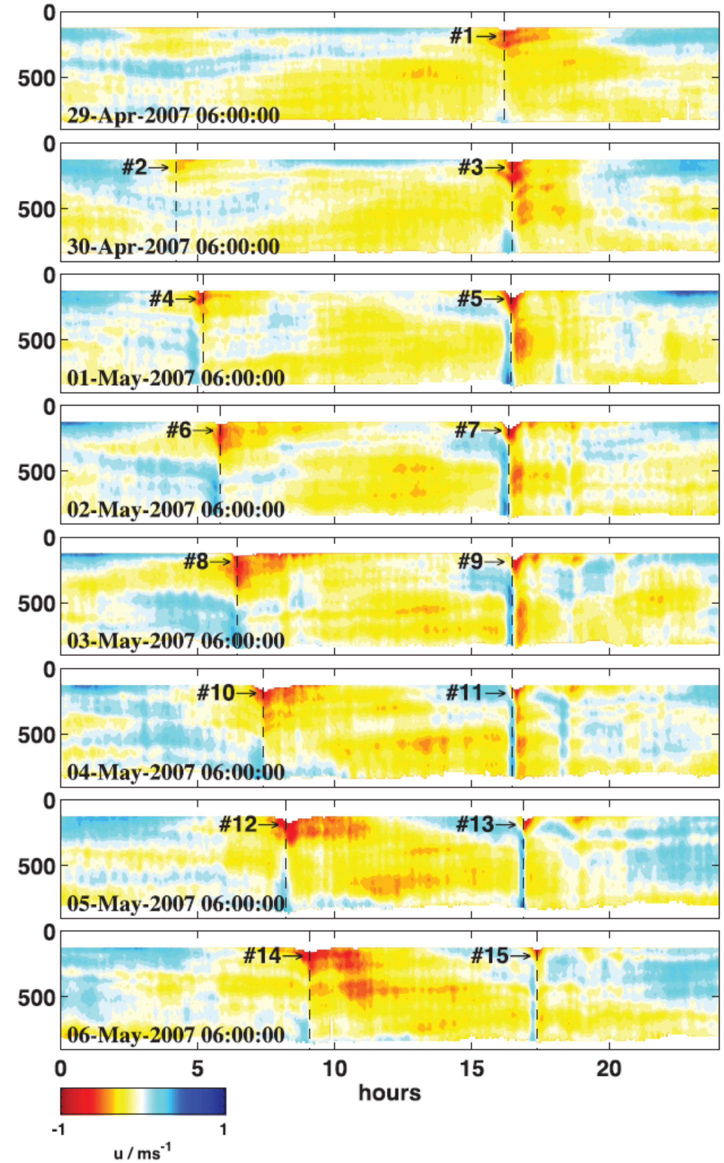

Ramp et al., IEEE J. Ocean. Engineering, 2004.
Alford et al., Journal of Physical Oceanography, 2010.

Observational evidence of A-type and B-type internal waves

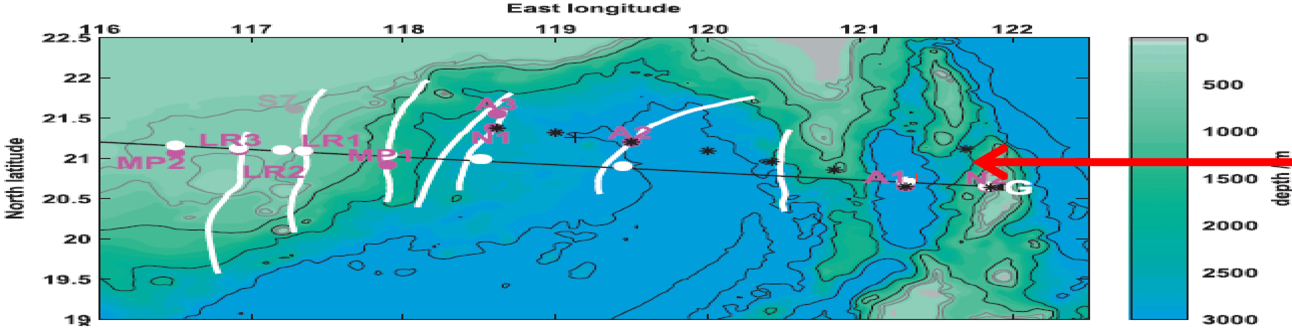

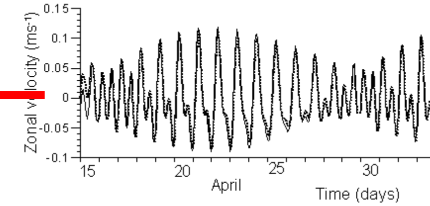

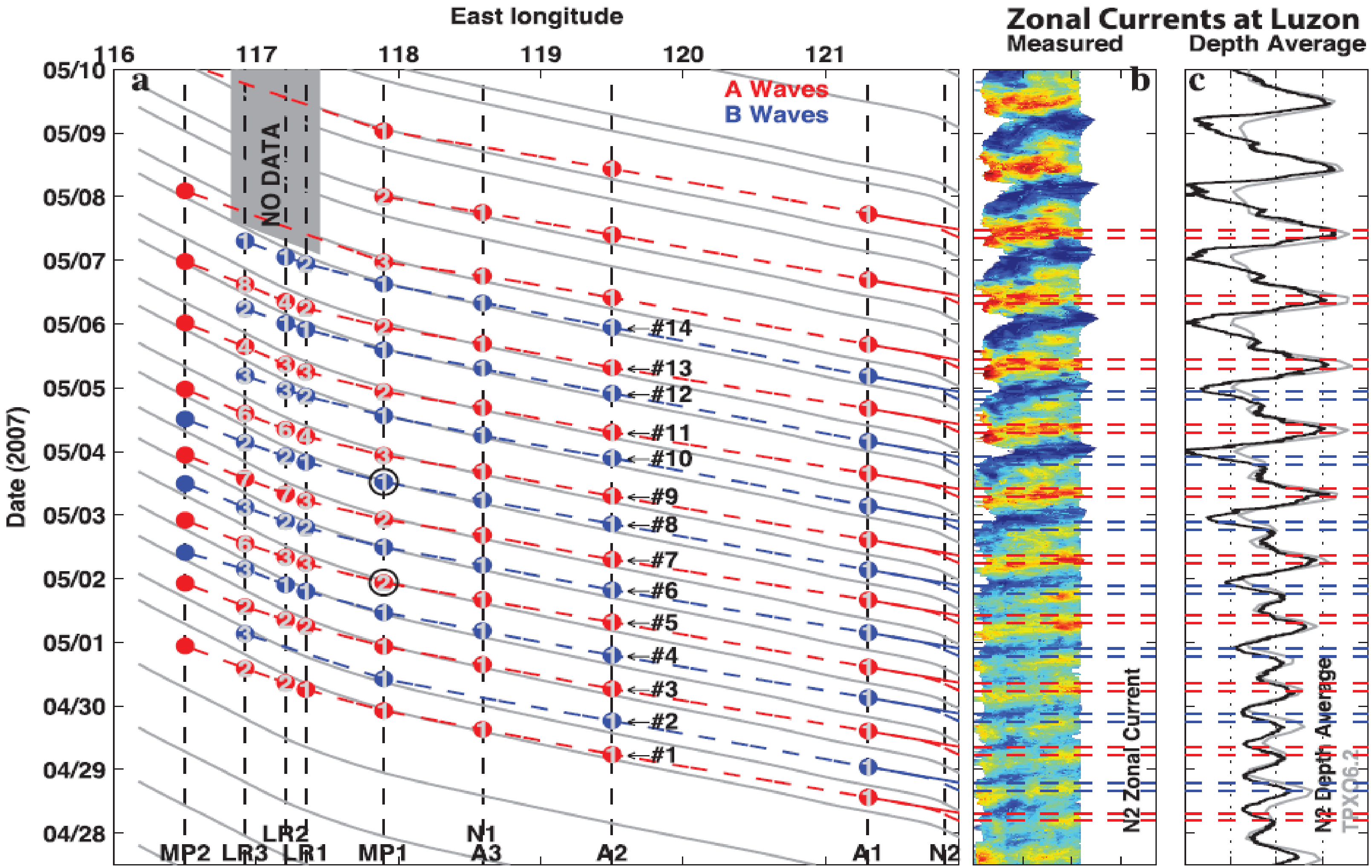

2. Analysis of some historical data: point M

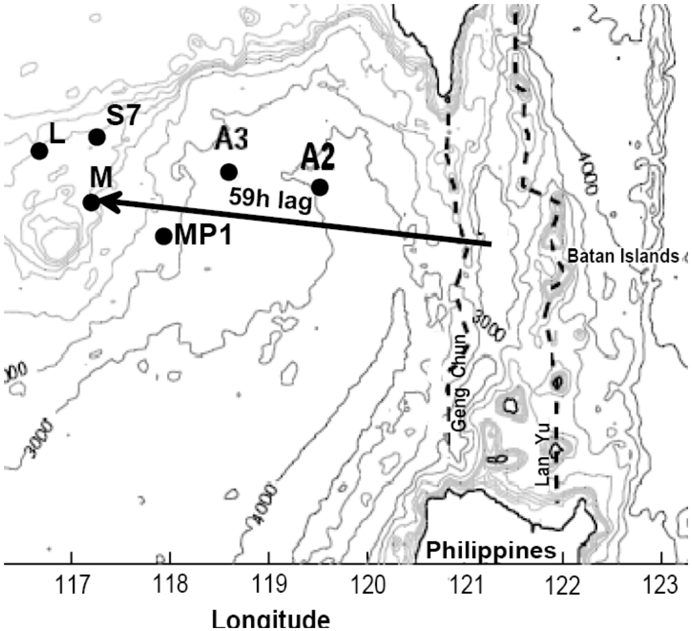

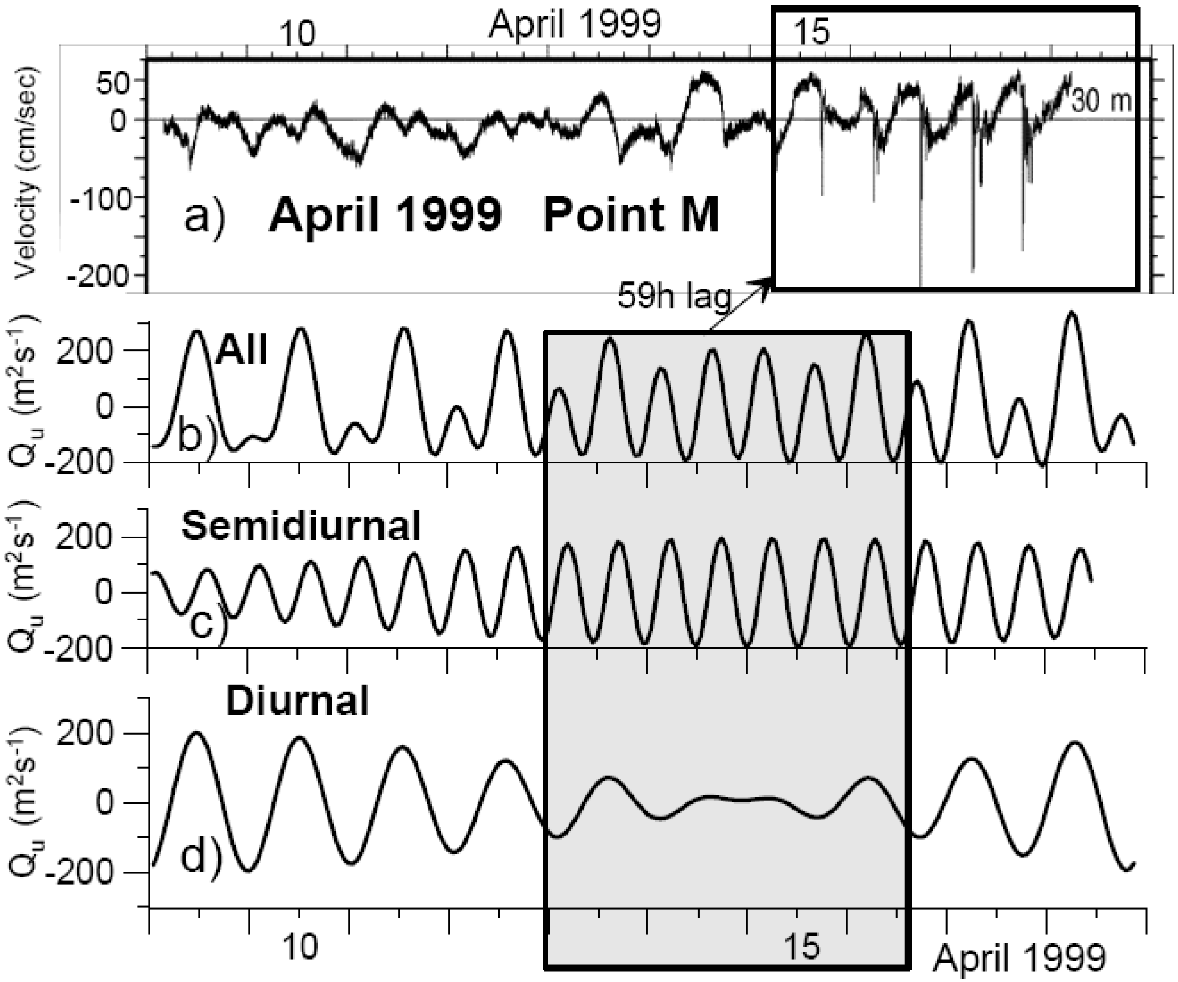

Yang, Y.-J., Tang, T. Y., Chang, M. H., Liu, A. K., Hsu, M.-K., Ramp, S.R., 2004. Solitons northeast of Tung-Sha Island during the ASIAEX pilot studies. IEEE J. Ocean. Engineering 29(4), 1182-1315.

Analysis of some historical data: Point L

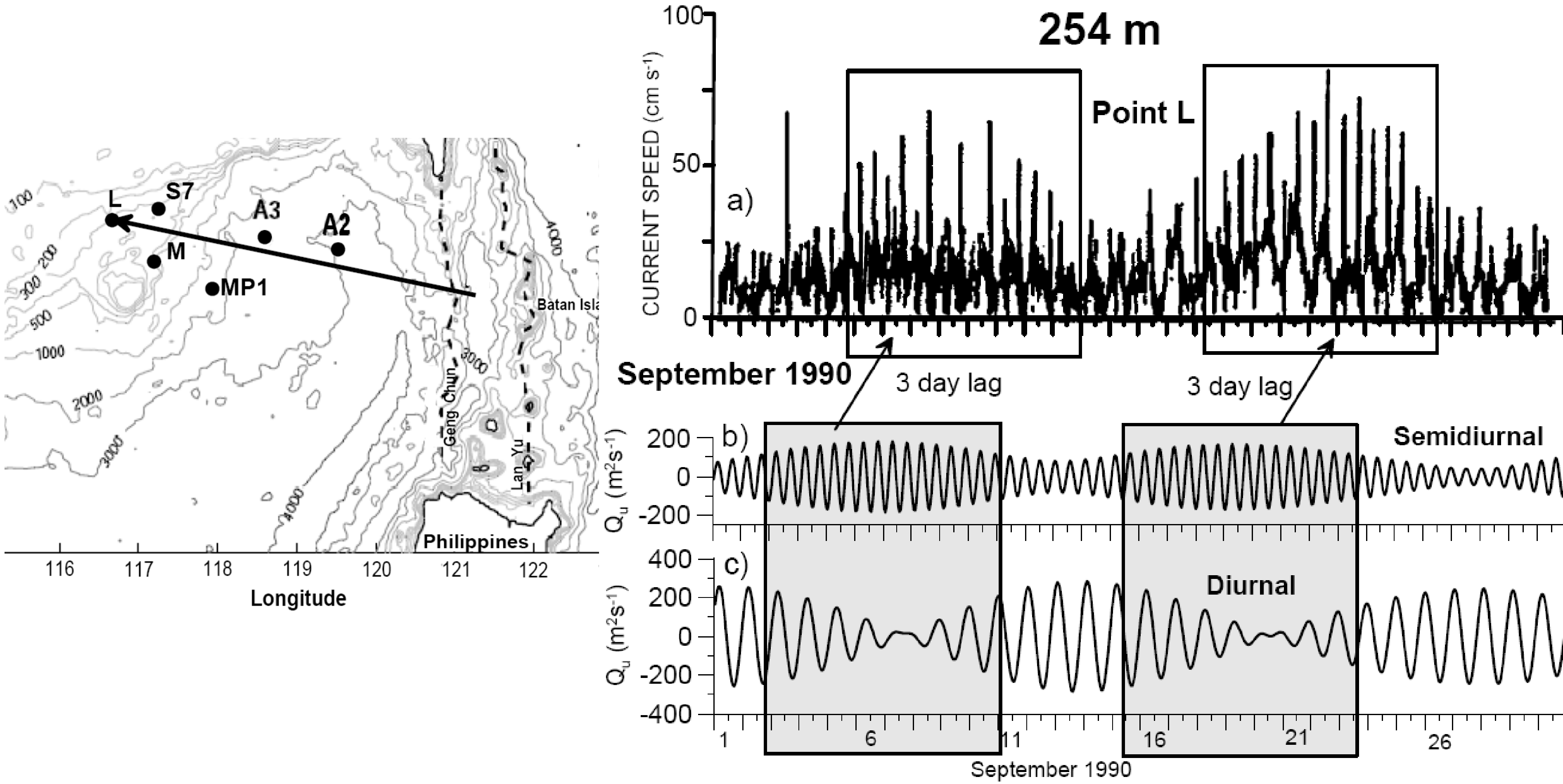

Ebbersmeyer, C.C., Coomes, C.A., Hamilton, R.C., Kurrus, K.A., Sullivan, T.C.,Salem B.L.,Romea, R.D., Bauer, R.J., 1991. New observations of internal waves (solitons) in the South China Sea using an acoustic Doppler current profiler In: Proceedings of Marine Technology Society Conference, New Orleans, May 1991, 165-175.

Analysis of some historical data: Point S7

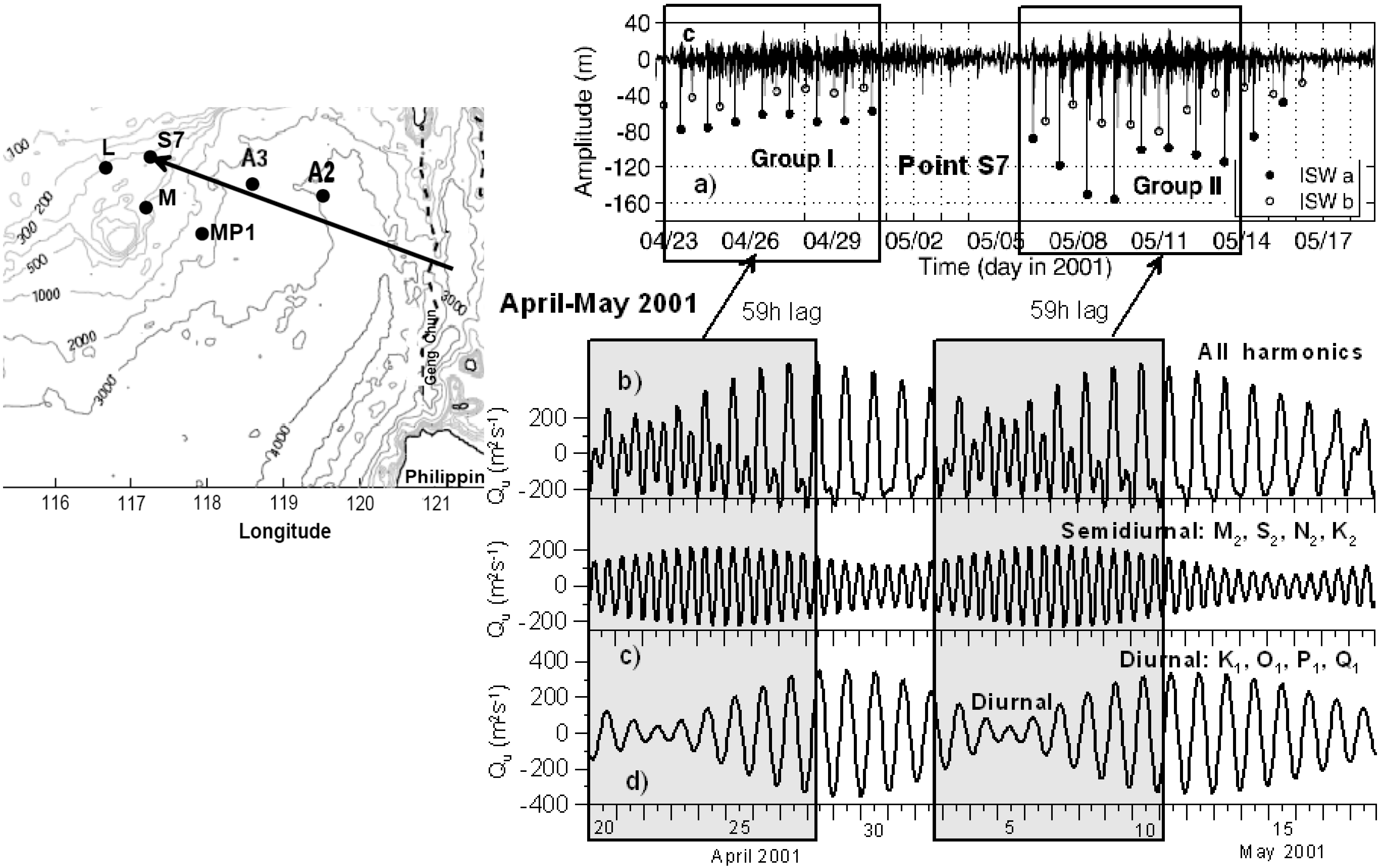

Zhao, Z., Alford, M. H., 2006. Source and propagation of internal solitary waves in the northeastern South China Sea. Journal of Geophysical Research 111, C11012, doi:10.1029/2006JC003644.

Analysis of some historical data: Point A2

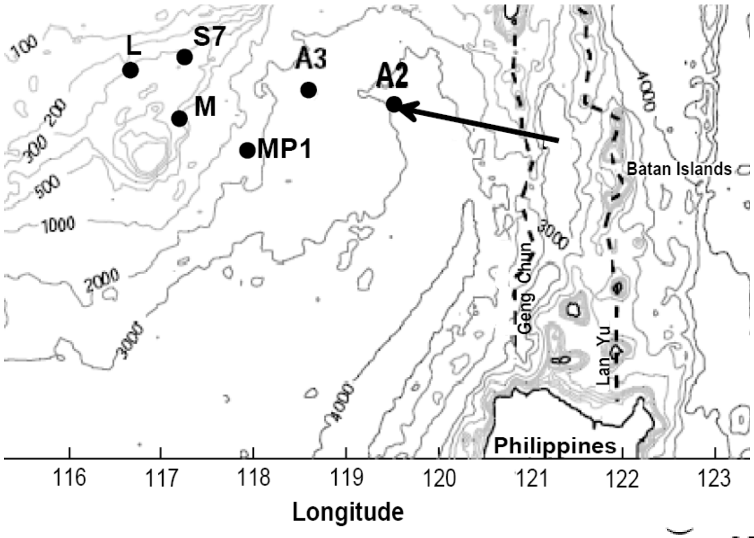

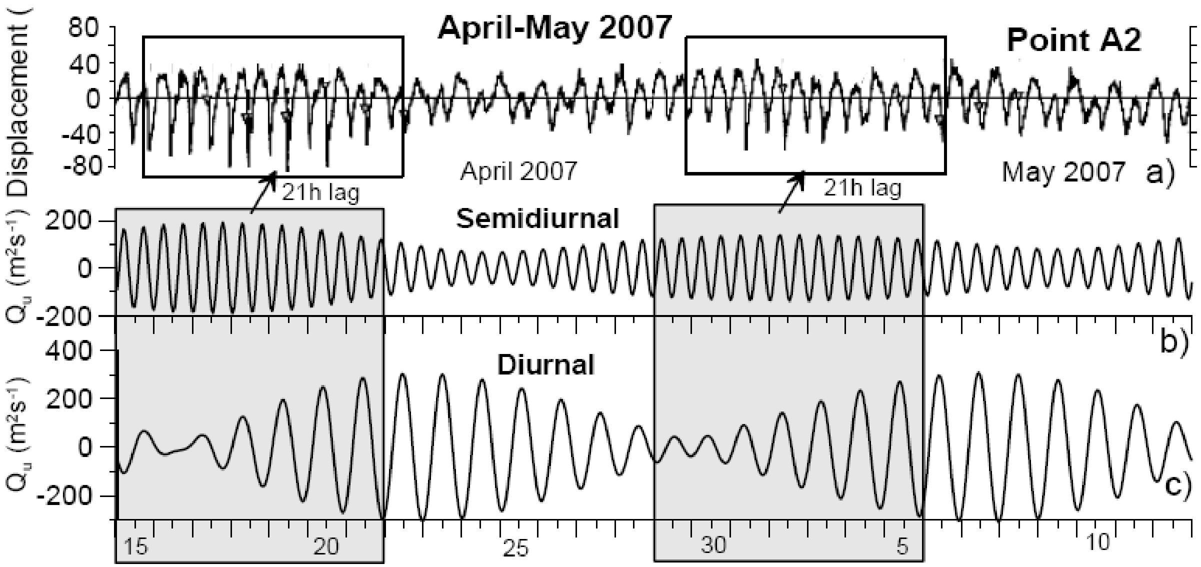

Farmer, D., Li, Q., Park, J.-H., 2009. Internal wave observations in the South China Sea: the role of rotation and non-linearity. Atmos.-Ocean 47(4), 267-280.

3. MITgcm modelling of A and B internal waves

- Model set-up
- Comparison with observational data

3. MITgcm modelling of A and B waves: Model set-up

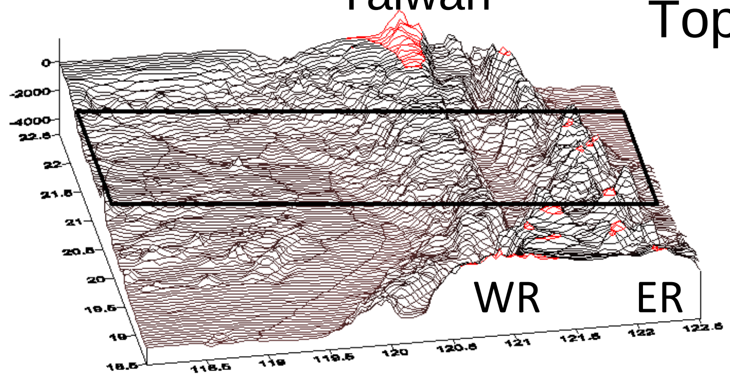

Topography

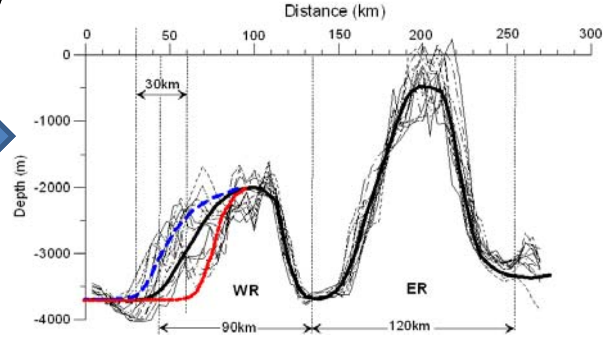

Stratification

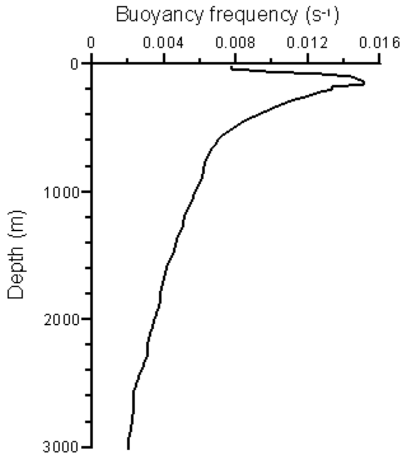

Forcing

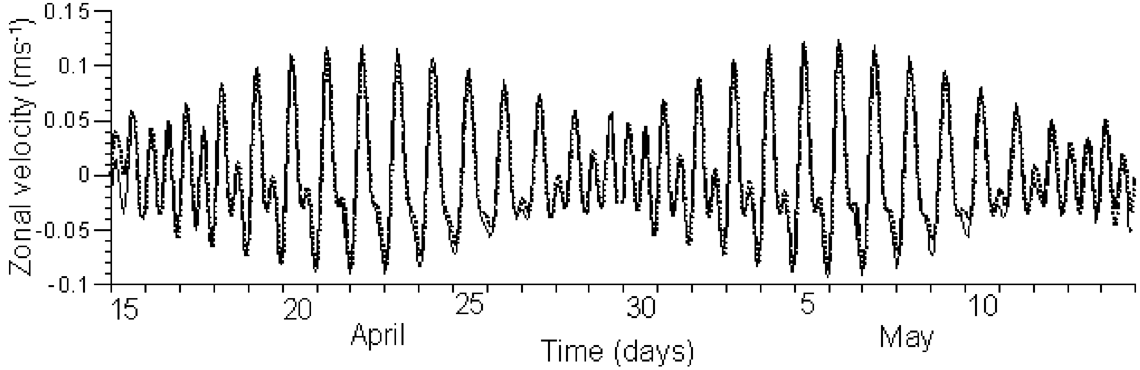

Resolution: Grid in horizontal direction: Δx=250 m;

Grid in vertical direction: Δz=10 m in upper 500 m; Δz=20 m for the next 20 layers; Δz=150m in the bottom layers.

3. MITgcm modelling of A and B waves: Results

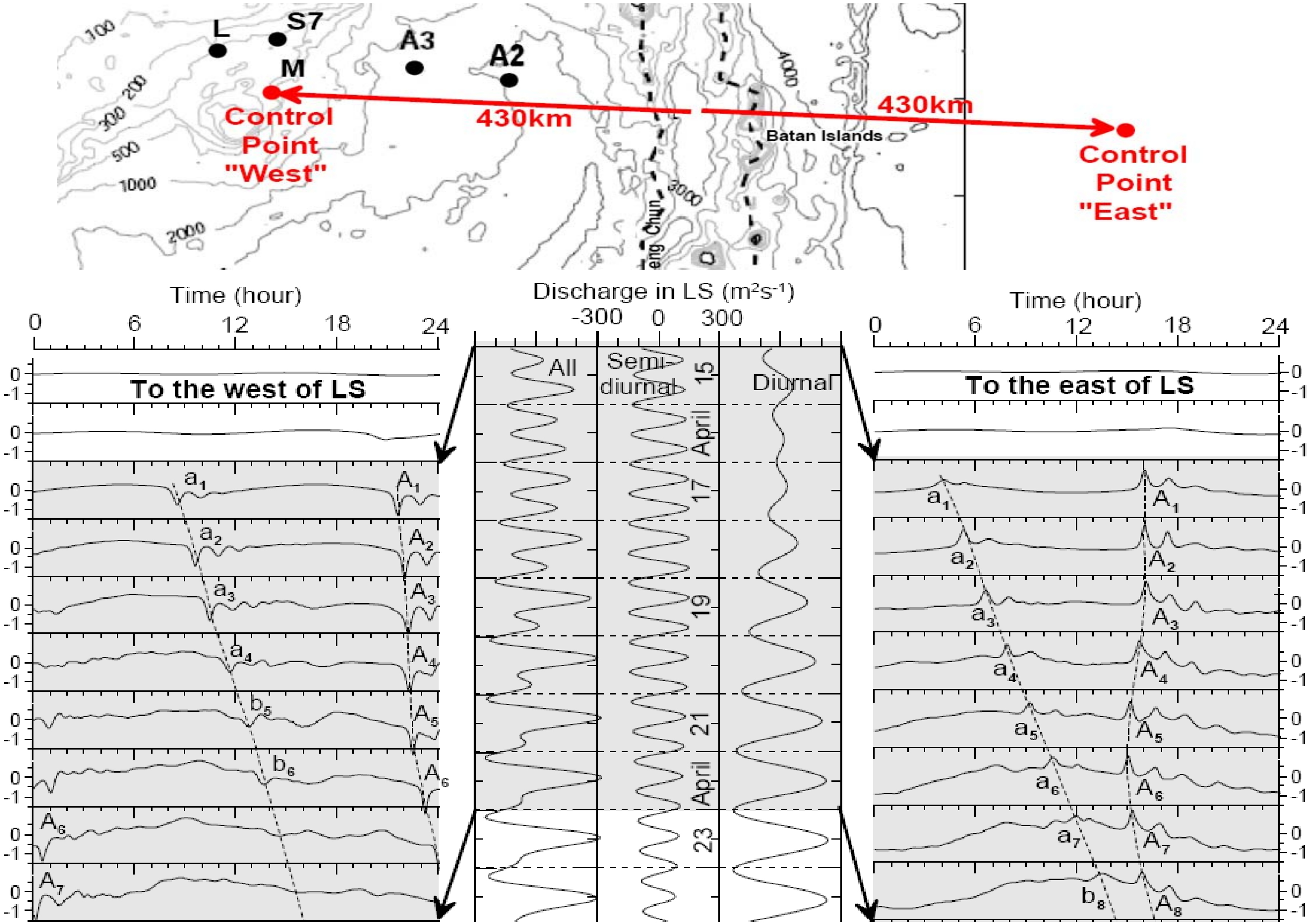

Time series of horizontal velocity on the surface $u(x_a,0,t)$ at two control points, “West” and “East”.

3. Long-term MITgcm modelling of A and B waves: Results

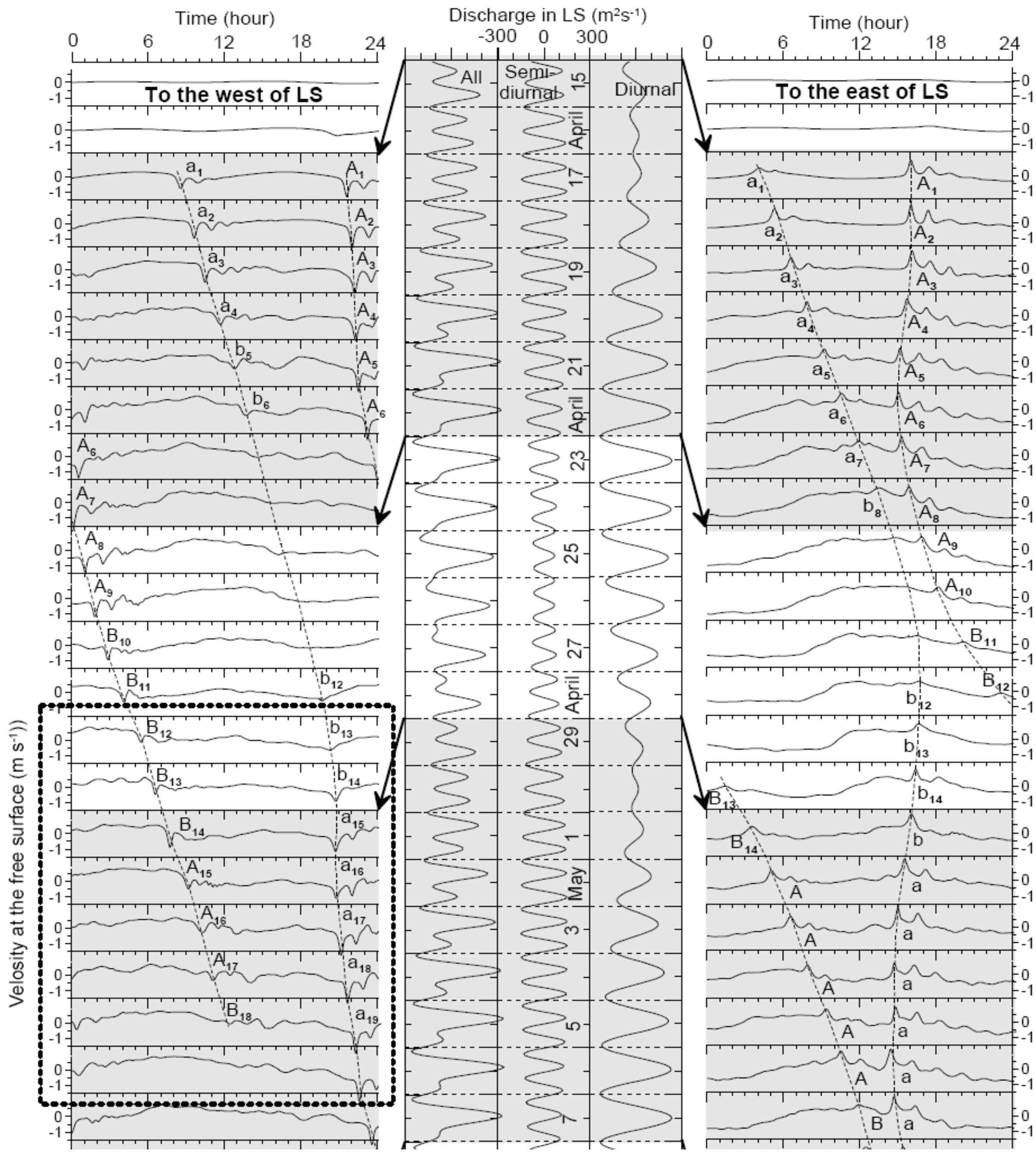

3. Comparison of the model output with observational data

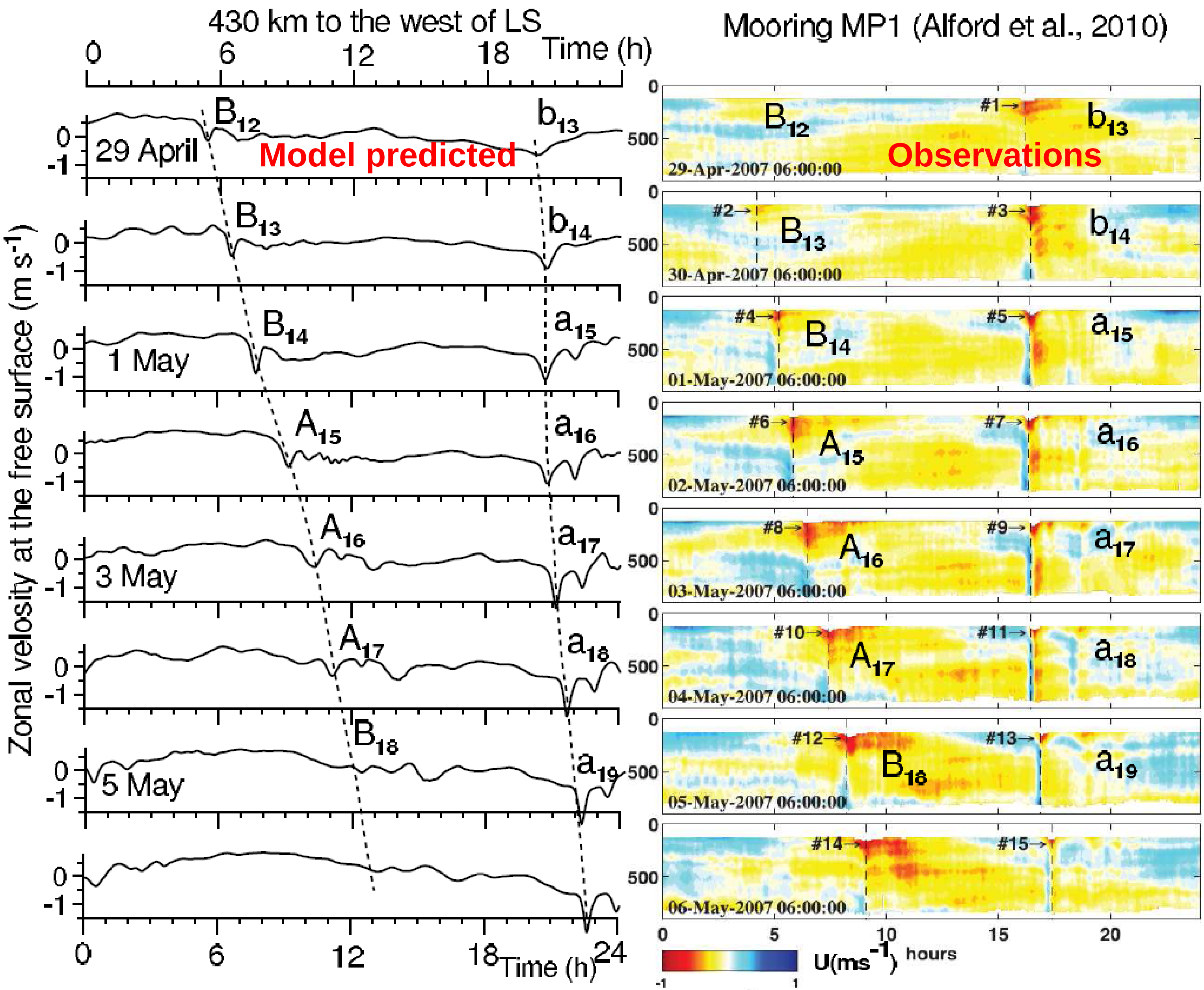

Alford et al., Journal of Physical Oceanography, 2010.

3. Comparison of the model output with observational data

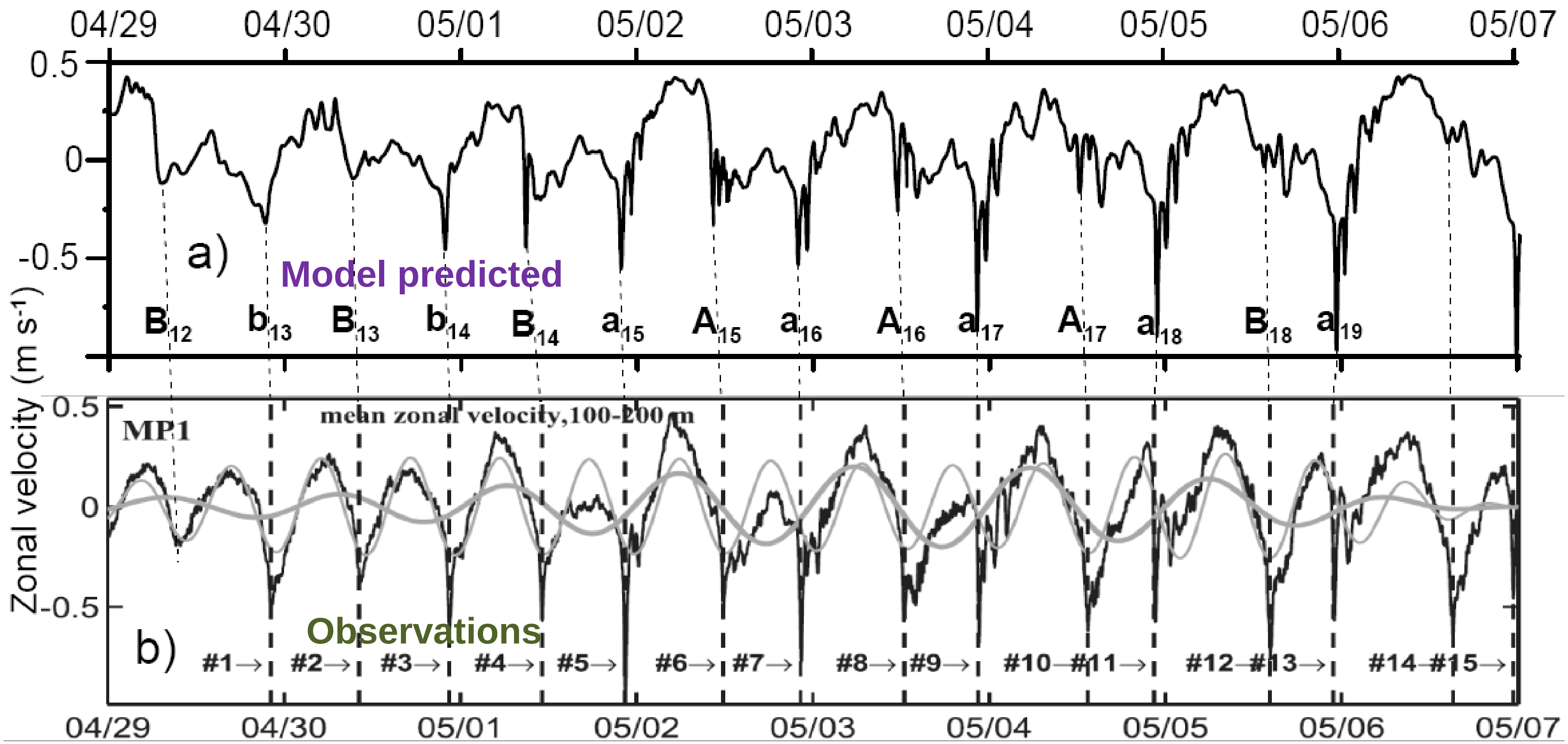

Alford et al., Journal of Physical Oceanography, 2010.

4. Analysis and interpretation of the model results

- Generation mechanism
- Multi-harmonic solution
- Evolutionary mechanism

4a. Generation mechanisms

$$\frac{dF}{dt} = \frac{\partial F}{\partial t} + U\frac{\partial F}{\partial x}$$

"Release" mechanism: Fr~1
Lee waves are generated downstream the ridge and radiated when flaw slackens

"Evolutionary" mechanism: Fr<<1
Steepening and disintegration of long internal tidal waves into packets of ISWs

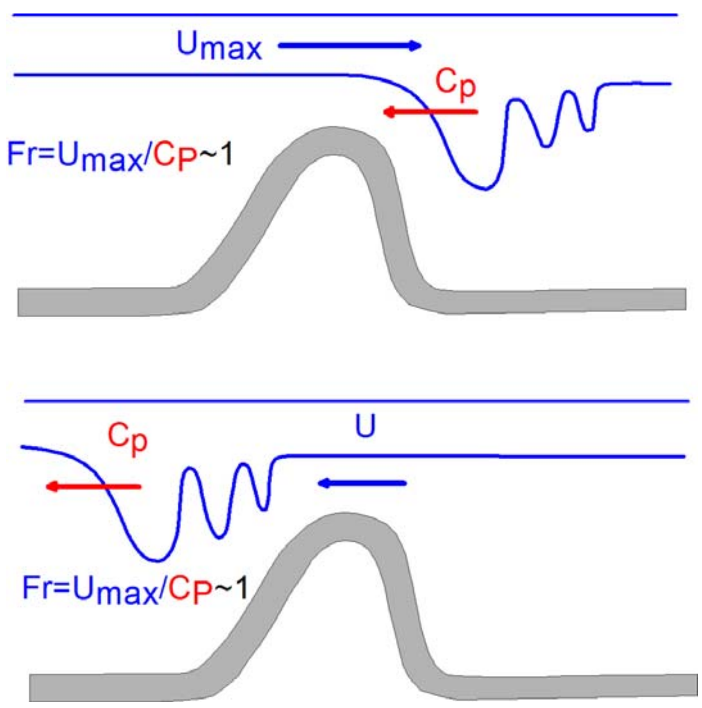

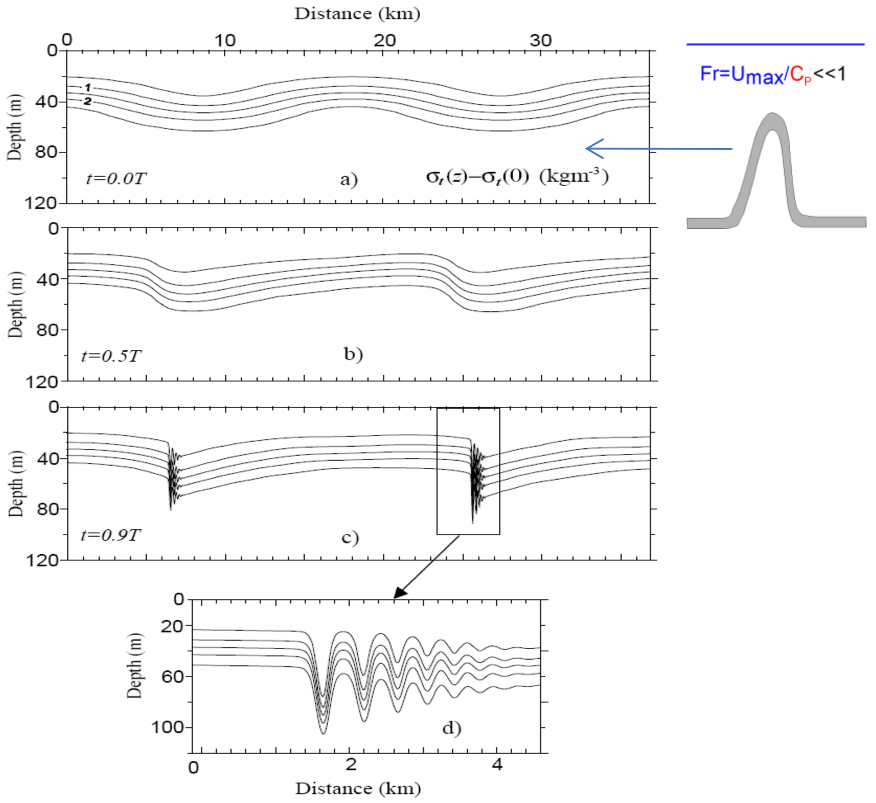

Linear theory prediction for ONE particular frequency σ

Analytical solution for idealised ridge
(Vlasenko et al. 2005)

$$\Psi_{xx} - \frac{\sigma^2 - f^2}{N^2(z) - \sigma^2}\Psi_{zz} = 0,$$

$$\Psi = \Psi_m, \quad z = 0,$$

$$\Psi = 0, \quad z = -H(x),$$

$$\Psi(x,z,t) = \Psi_m(1 + z/H)\exp(-i\sigma t) + \sum_{j=1}^{\infty} a_j g_j(z)\exp[i(k_j x - \sigma t + \varphi_j)].$$

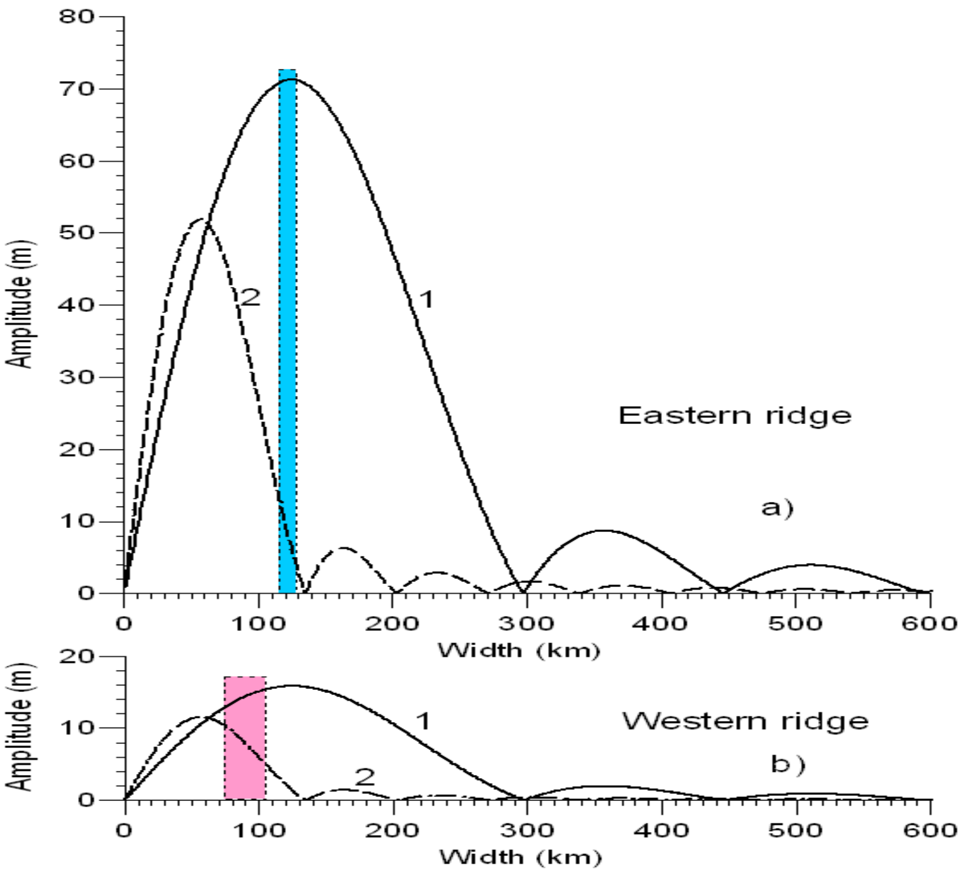

Resonant generation of modes

Second-mode amplitude for two ridges

Linear theory prediction for TWO tidal harmonics: semidiurnal and diurnal

Tidal forcing Q=200 m^2/sec=const, ridge width - variable

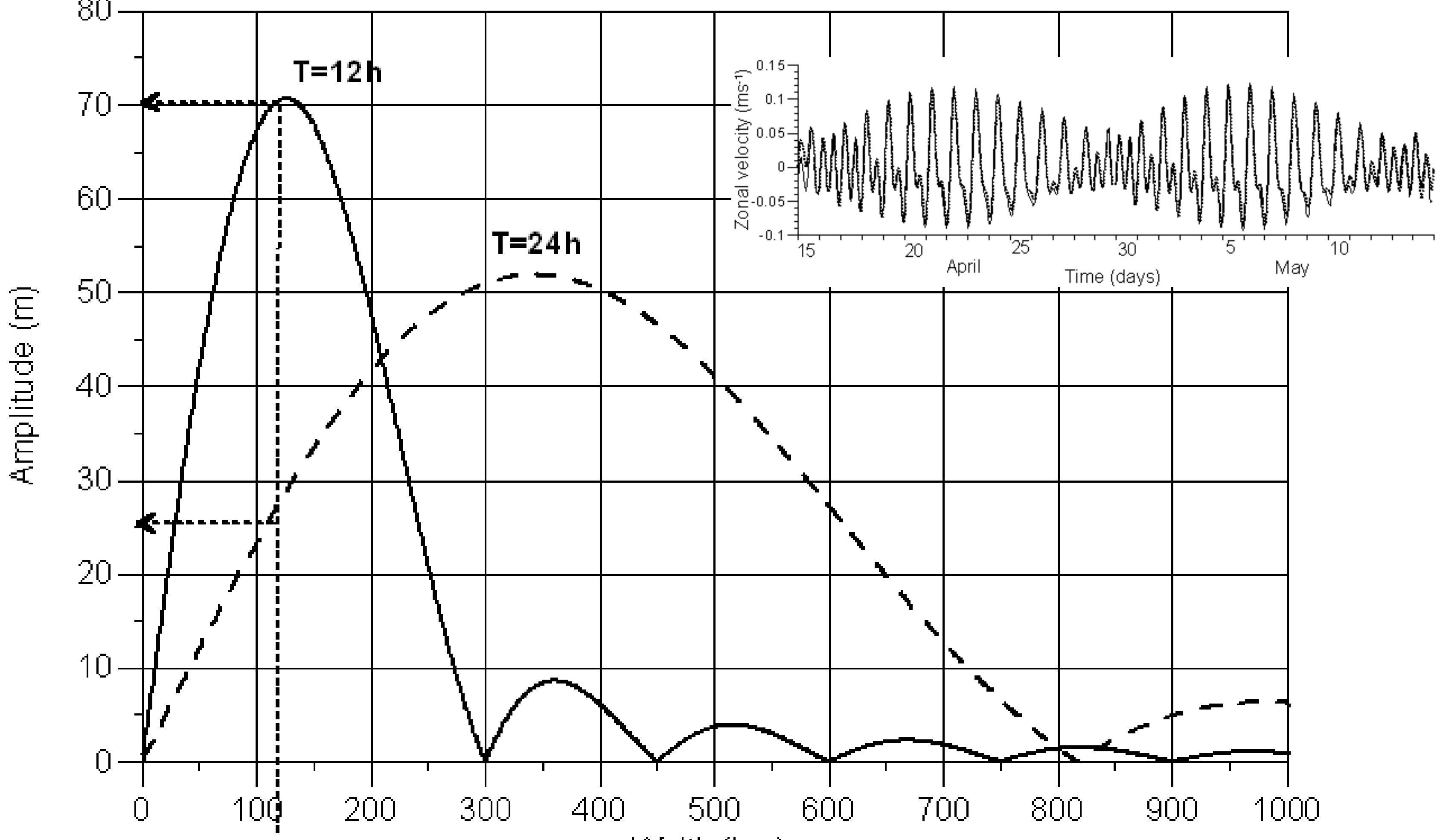

Linear theory prediction for the generation of the first-mode baroclinic tide in the South China Sea by the semidiurnal and diurnal barotropic tide (Q=200m^2/sec in the Luzon Strait)

Linear theory prediction for TWO tidal harmonics: semidiurnal and diurnal

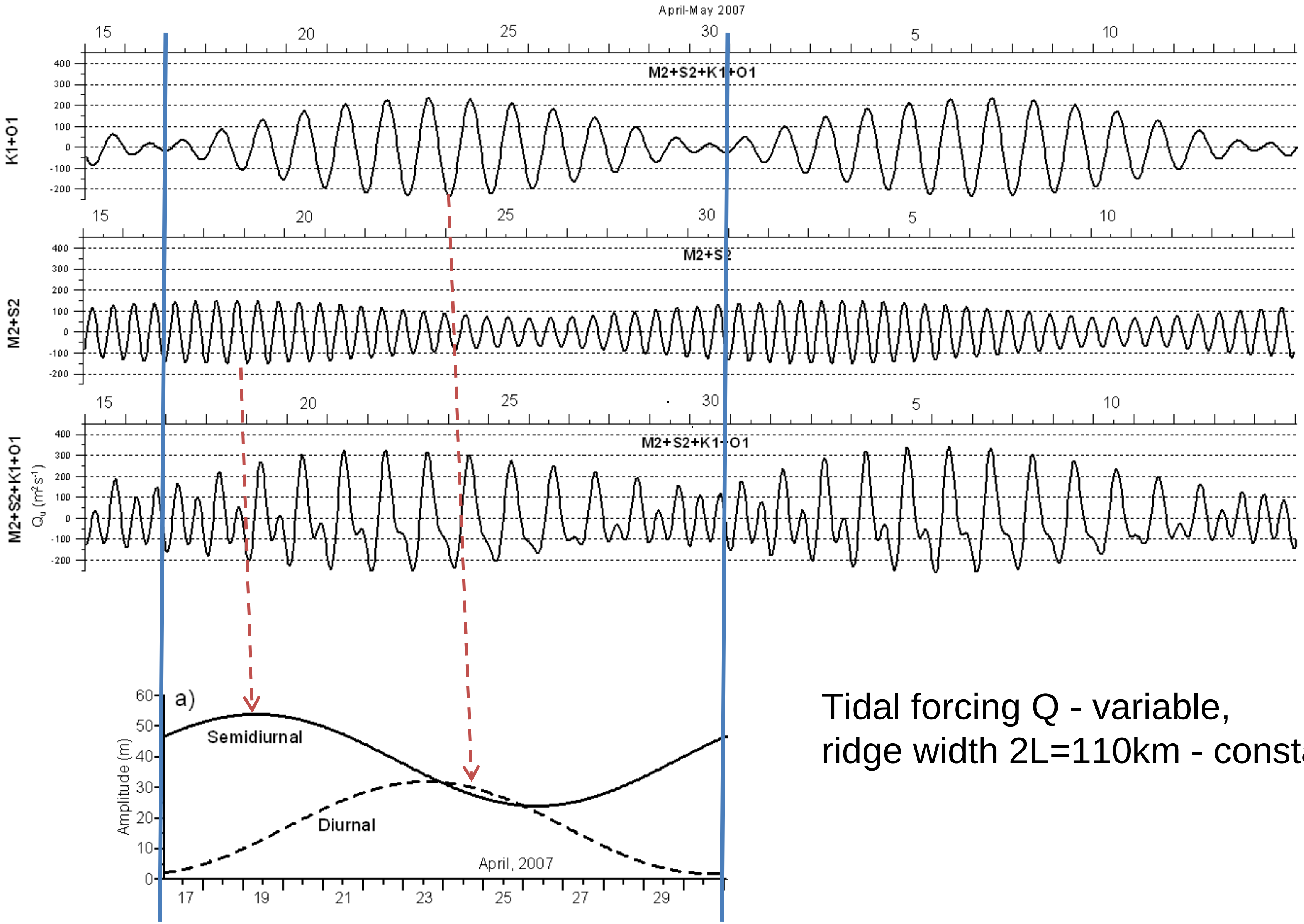

Tidal forcing Q - variable,
ridge width 2L=110km - constant.

Superposition of TWO tidal harmonics: semidiurnal and diurnal

$$\zeta(x,z,t) = a_1^s g_1(z)\exp(k_1^s x - \sigma^s t + \varphi_1^s) + a_1^d g_1(z)\exp(k_1^d x - \sigma^d t + \varphi_1^d)$$

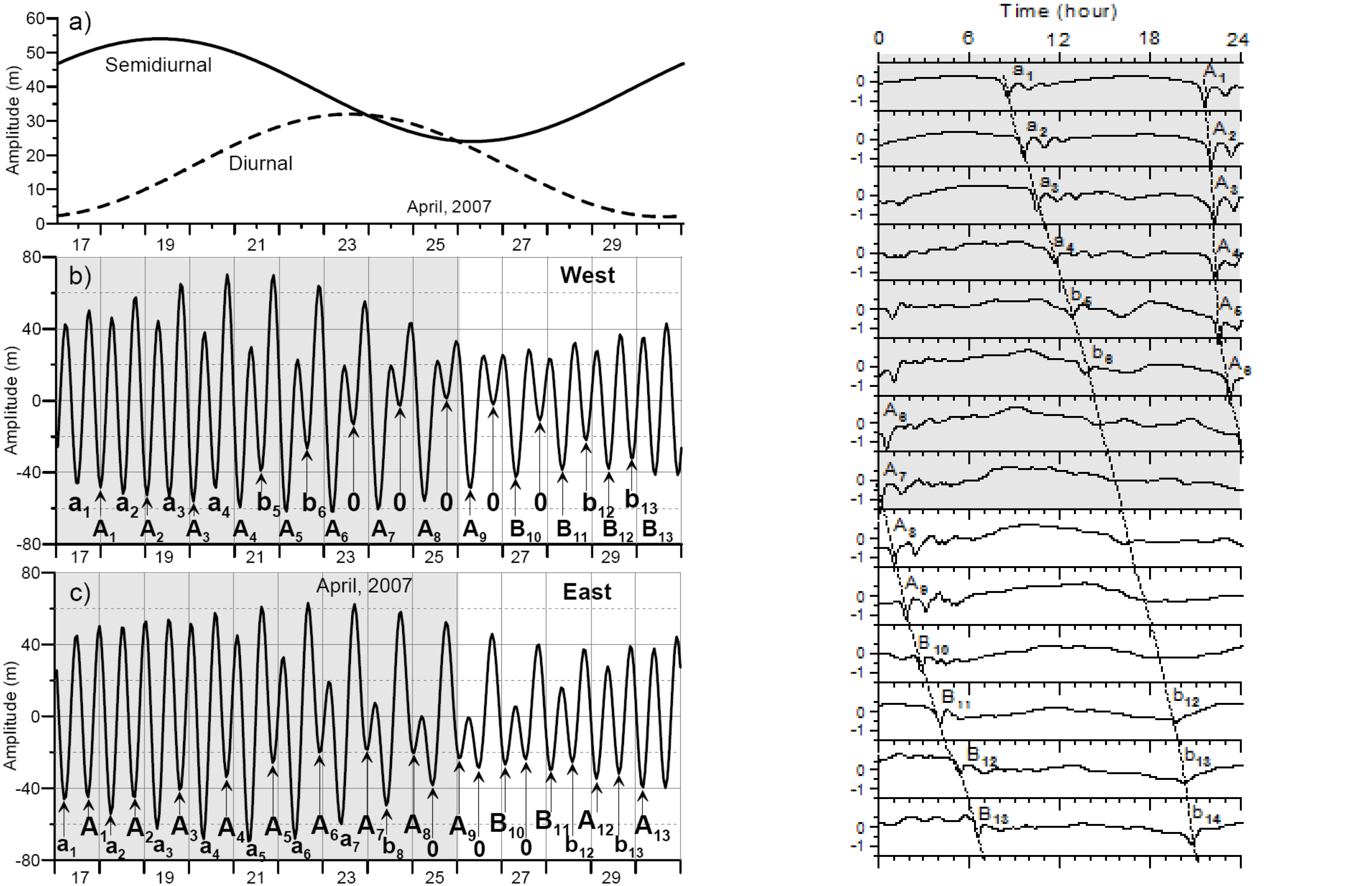

Evolutionary mechanism: steepening and disintegration into ISWs

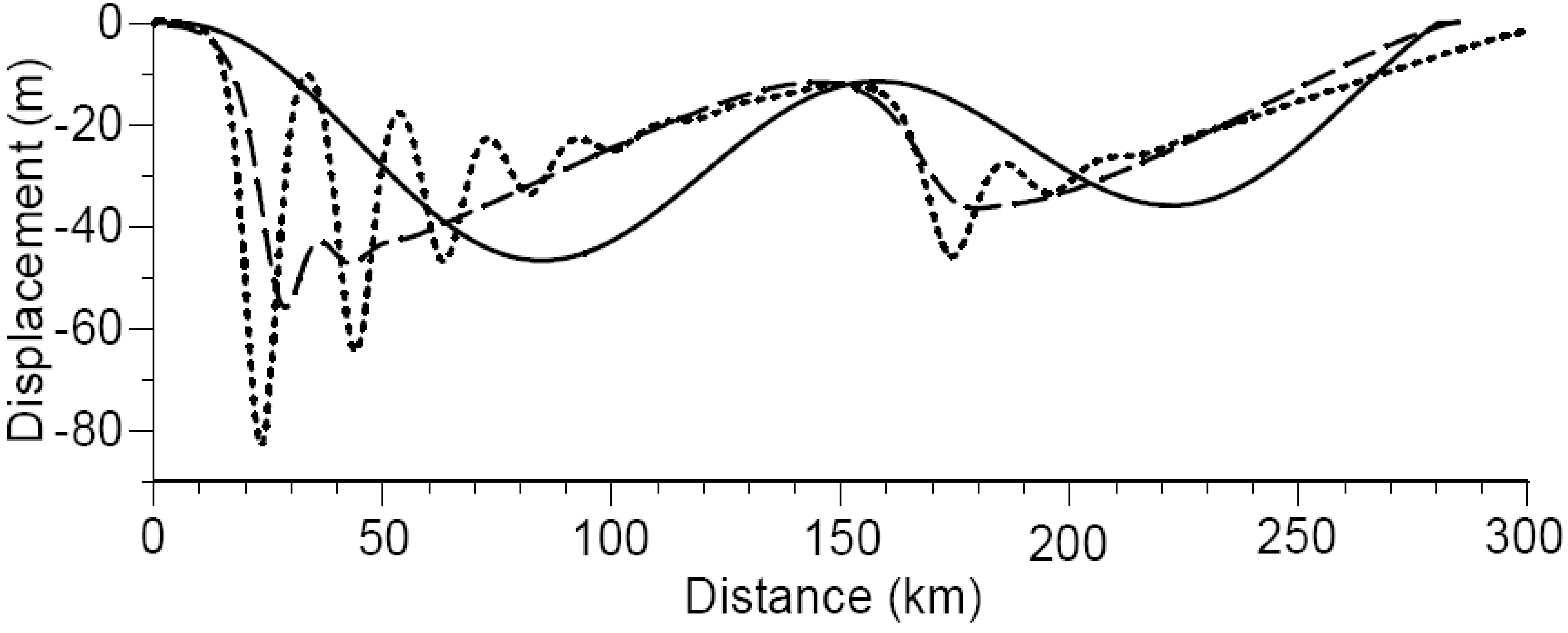

$$N < \frac{1}{2}[\sqrt{1 + \frac{6a\epsilon(1-2\alpha)}{\nu^2\delta}} + 1],$$

5. Conclusions

1. The amplitudes of ISWs is controlled by the intensity of semidiurnal tidal harmonics. Much stronger diurnal constituents do not reveal any substantial influence on the appearance of ISWs. This effect can be treated in terms of rotational dispersion.
2. The role of the diurnal tidal harmonics is in modulation of the generated internal waves. Diurnal periodicity is introduced into the ISW signal known as A and B waves. Appearance of A or B type waves is not directly linked to strong or weak tidal current peaks in the LS.
3. The MITgcm modelling shows that the number of ISWs in A and B wave packets varies with neap-spring periodicity with a gradual transition of A waves into B waves, and vice versa. The arrival time of A and B waves at observational point varies both for A and B packets depending on the forcing conditions in the LS.
4. The effect of A-B-A-B wave transition can be treated in terms of a multi-harmonic evolutionary mechanism. Generated in the LS semidiurnal and diurnal internal tidal harmonics freely radiate from the ridge. Being superimposed, these two progressive waves produce an intermittent baroclinic signal with large and small wave troughs alternating in space and time. In the course of nonlinear evolution these large and small wave troughs steepen and ultimately disintegrate into A and B wave packets.